Subterranean Biology 34: 61–98 (2020)
doi: 10.3897/subtbiol.34.49586
http://subtbiol.pensoft.net

RESEARCH ARTICLE

A peer-reviewed open-access journal
Subterranean Biology
Published by The International Society for Subterranean Biology

Cave-dwelling pseudoscorpions of China with descriptions of four new hypogean species of *Parobisium* (Pseudoscorpiones, Neobisiidae) from Guizhou Province

Zegang Feng[1], J. Judson Wynne[2], Feng Zhang[1]

1 *The Key Laboratory of Zoological Systematics and Application, College of Life Sciences, Hebei University, Baoding, Hebei 071002, China* **2** *Department of Biological Sciences, Colorado Plateau Museum of Arthropod Biodiversity and Merriam-Powell Center for Environmental Research, Northern Arizona University, Flagstaff, Arizona 86011, USA*

Corresponding author: Feng Zhang (dudu060420001@163.com)

Academic editor: O. Moldovan | Received 23 December 2019 | Accepted 22 February 2020 | Published 26 March 2020

http://zoobank.org/3FD733A3-F576-42AC-9ACA-7CAF915DD82C

Citation: Feng Z, Wynne JJ, Zhang F (2020) Cave-dwelling pseudoscorpions of China with descriptions of four new hypogean species of *Parobisium* (Pseudoscorpiones, Neobisiidae) from Guizhou Province. Subterranean Biology 34: 61–98. https://doi.org/10.3897/subtbiol.34.49586

Abstract

We summarize and discuss the 29 known cave-dwelling pseudoscorpion species from China. Four new troglomorphic pseudoscorpion species, *Parobisium motianense* **sp. nov.**, *P. qiangzhuang* **sp. nov.**, *P. sanlouense* **sp. nov.**, and *P. tiani* **sp. nov.**, belonging to the family Neobisiidae, are described based on specimens collected in karst caves in Guizhou, China. Detailed diagnosis, descriptions, and illustrations are presented. We also provide recommendations for management of caves where they occur, as well as the cave arthropod communities and the habitats that support them.

Keywords

cavernicoles, cave conservation, taxonomy, troglobionts

Introduction

Biospeleological studies in the South China Karst (SCK) has rapidly accelerated in recent years. Since 2017, 39 new subterranean-adapted species across several taxonomic arthropod groups have been described (Gao et al. 2017; Huang et al. 2017; Li and Wang 2017; Song et al. 2017; Tian et al. 2017, 2018; Deuve and Tian 2018; Li et al. 2019a). Overall, at least 382 cave-dwelling arthropod species are now known from this region (Ran and Yang 2015; Tian et al. 2016; Li and Wang 2017; Gao et al. 2018; Feng et al. 2019; Li et al. 2019b; Liu and Wynne 2019). Incidentally, this work has also resulted in the identification of at least 21 troglomorphic pseudoscorpion species (refer to Feng et al. 2019; Li et al. 2019b).

In the last 25 years, cave-dwelling pseudoscorpions from China, specifically in Guizhou, Yunnan, Guangxi, Sichuan, and Hubei Provinces, and Beijing and Chongqing Municipalities, total at least 29 pseudoscorpion species (Schawaller 1995; Mahnert 2003, 2009; Mahnert and Li 2016; Gao et al. 2017; Li et al. 2017; Gao et al. 2018; Feng et al. 2019; Li et al. 2019; Table 1). Of these, 23 are troglobionts and six are troglophiles (Table 1). With 18 species, Neobisiidae is the most diverse family with species spanning two genera: *Parobisium* Chamberlin, 1930 and *Bisetocreagris* Ćurčić, 1983. Additionally, the families Chernetidae and Chthoniidae contain six and five species, respectively.

The pseudoscorpion genus *Parobisium* was first established by Chamberlin (1930) as a subgenus of *Neobisium* Chamberlin, 1930, and later elevated by Chamberlin and Malcolm (1960) to generic rank. *Parobisium* is characterized by the absence of a galea on the movable cheliceral finger, fixed chelal finger with a compact subterminal cluster of only three tactile setae (*et*, *it*, *est*), and a more diffuse subbasal to basal cluster of five tactile setae (*isb*, *ist*, *ib*, *esb*, *eb*) (Chamberlin 1962). However, for some North American and Asian *Parobisium* species, the trichobothrium (*est*) is isolated in the distal half of the fixed finger and has a trichobothrial pattern quite similar to *Bisetocreagris*.

The key character used to distinguish between these two genera is that *Bisetocreagris* usually has elongate galeae. Mahnert and Li (2016) intimated the galea is extremely fragile in *Bisetocreagris* species. This implies galea may be easily broken or damaged during collection or transport (Y. Li, pers. com., 18 December 2019). Subsequently, using galeae as a diagnostic character for describing and identifying species may hinder accurate classification of this group. In general, *Parobisium* differs from *Bisetocreagris* as there is a distinct and rounded sclerotic knob, rather than an absence of galea (Morikawa 1960; Hong 1996; Mahnert and Li 2016).

During the examination of Guizhou specimens collected by Mingyi Tian (of the South China Agricultural University, Guangzhou Province) between 2013 and 2017, we identified several species of *Parobisium*, which may be undescribed. In most cases, we had too few specimens to formally describe the species, and in some cases we had only one specimen. Unfortunately, this can be limiting in describing new species, especially given the aforementioned considerations with the galea. To address this problem, the lead author and colleagues collected additional specimens at the

caves originally sampled by M. Tian. With additional specimens, we were able to both describe these species and confirm that these *Parobisium* species have a distinct and rounded sclerotic knob rather than the absence of galae.

Based upon specimens collected by both M. Tian and the lead author, we describe four new species of *Parobisium* from caves in Guizhou Province, China. All species are subterranean-adapted, and include *P. motianense* sp. nov., *P. qiangzhuang* sp. nov., *P. sanlouense* sp. nov., and *P. tiani* sp. nov. We also provide recommendations for management of these caves and the cave arthropod communities and habitats they support.

Material and methods

Study area

Guizhou, located in the Yunnan-Guizhou Plateau, is the centrally located province within the SCK. The karst escarpment within this area is approximately 130,000 km^2 encompassing 73% of Guizhou Province (Rong and Yang 2004; He and Li 2016). Karst formation in Guizhou emerged from a plate group from the Proterozoic to the Quaternary Period, and consists mainly of shallow marine carbonate deposits (Zhou et al. 2017). The extensive distribution of carbonate geology and the subtropical monsoon climate provide suitable conditions for the development of karst caves. According to Zhou et al. (2017), Guizhou supports at least 4,960 caves.

The lead author and colleagues searched for and collected pseudoscorpions within three of the four Guizhou caves (Fig. 1) where M. Tian initially collected specimens. As none of these caves were subject to previous studies or exploration efforts, cave maps were not available. We have provided estimations of entrance configuration and cave length, as well as information on surface vegetation and adjacent human activities.

Motian Cave (Figs 1C, 18) is located ~2 km southwest of Tangbian Town, Pingtang County. This limestone cave has one downward sloping oval entrance (~8 meters high by ~4 meters wide), approximately 2100 meters in length, and extends horizontally. The cave is surrounded by agriculture with the nearest rural residential area less than 100 m from the cave entrance.

Zharou Cave (Figs 1B, 19) is located ~1 km north of Daying Town, Ziyun County. This limestone cave has one triangular entrance (~2 meters high and ~3.5 meters wide), approximately 80 meters in length, and extends horizontally. The surrounding area is largely disturbed and characterized by low shrubs and weeds (Gramineae); agricultural fields and a rural residential area are approximately 100 m away.

Sanlou Cave (Figs 1D, 20) is located ~2.5 km northwest of Daoping Town, Fuquan City. This horizontally-trending cave is approximately 200 meters in length and has an irregularly round entrance (~4 meters in diameter). Situated near a sand mining operation, this cave is the primary water source for the village of Daoping. Subsequently, a reservoir and water delivery system was built in the deepest part of the cave. The cave has also been designated as a water source protection area.

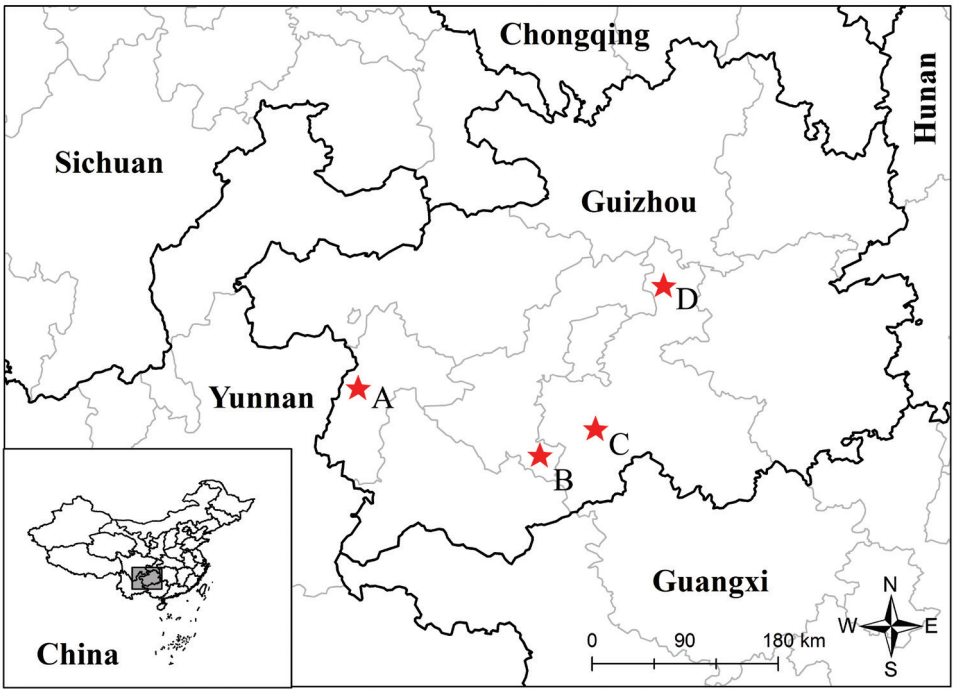

Figure 1. Study area, general cave locations, and type locality for each species, Guizhou Province, China. **A** Biyun Cave, *Parobisium tiani* sp. nov. **B** Zharou Cave, *Parobisium qiangzhuang* sp. nov. **C** Motian Cave, *Parobisium motianense* sp. nov. **D** Sanlou Cave, *Parobisium sanlouense* sp. nov.

Biyun Cave (Figs 1A, 21) is located in Biyun Park, Chengguan Town, Pan County and is less than 50 m from a rural residential area. This cave has two entrances. One entrance is dome-shaped (~30 meters wide at the base and 10 m high); during the rainy season, a river flows into this cave entrance. The second entrance is located about 80 m uphill from the lower entrance and is irregularly round in shape (~30 meters in diameter). This cave was developed as a tourist cave, and has an unmaintained footpath paved with concrete, which connects the two entrances.

Field sampling

From 29 July to 5 August 2019, researchers conducted direct intuitive searches (*sensu* Wynne et al. 2019) in the estimated deep zone of each cave by examining bat guano, dead insects, edges of pools and streams, flood detritus, and mud floors (Figs 19B, 20C). Two observers spent approximately two hours searching in Zharou Cave, four hours searching in Biyun cave, and four observers spent about three hours searching Sanlou Cave.

Preparation and analysis

Specimens were preserved in 75% ethanol and deposited in the Museum of Hebei University (MHBU), Baoding, China. Photographs were taken using a Leica M205A stereomicroscope equipped with a Leica DFC550 camera and LAS software (Ver. 4.6). We used a Leica M205A stereomicroscope (with a drawing tube) for drawings and measurements. Chela and chelal hand were measured in ventral view. All measurements are in millimeters (mm) unless noted otherwise. Detailed examination of characters was done using an Olympus BX53 general optical microscope. Temporary slide mounts were prepared in glycerol.

Terminology

Cave ecosystems typically consist of four environmental zones (Howarth 1980, 1983): (1) *entrance zone*—or light zone, which represents a combination of surface and cave environmental conditions; (2) *twilight zone*—occurring slightly deeper within the cave and has both diminished light conditions and direct influence of surface environment; (3) *transition zone*—aphotic, yet barometric and diurnal shifts may still occur at a significantly diminished rate, but the climate is approaching near stable conditions; and, (4) *deep zone*—complete darkness, high environmental stability, near stable temperature, near water-saturated atmosphere, and low to no airflow (usually in the deepest part of the cave). The deep zone represents the region most conducive to supporting subterranean-adapted animals. Although there are four primary cave specific functional groups recognized, the species discussed here have been identified as either *troglobionts* or *troglophiles*. Troglobionts are obligate cave dwellers that require the stable environmental conditions of the deep zone to complete their life cycle and exhibit morphological characteristics (i.e., troglomorphisms) indicative of subterranean adaptation (Sket 2008). Troglophiles (or *troglophilous* organisms) lack troglomorphic characters yet occur facultatively within caves and complete their life cycles there, but also occur in similar cave-like surface habitats (Barr 1967, Howarth 1983).

Pseudoscorpion terminology and measurements mostly follow Chamberlin (1931) with some minor modifications to the terminology of the trichobothria (Harvey 1992) and chelicera (Judson 2007). The following abbreviations used for the trichobothria: *b* = basal; *sb* = sub-basal; *st* = sub-terminal; *t* = terminal; *ib* = interior basal; *isb* = interior sub-basal; *ist* = interior sub-terminal; *it* = interior terminal; *eb* = exterior basal; *esb* = exterior sub-basal; *est* = exterior sub-terminal; and, *et* = exterior terminal.

Table 1. The 29 known cave-dwelling pseudoscorpion species from China. 'Category' indicates the functional group in which each species belongs – either troglobiont or troglophile. The number of caves (# Caves) may be used to infer the level of endemism. Names of administrative provinces where each species is presently known is also provided.

Taxa	Category	#Cave	Province	Reference
Family Chernetidae				
Megachernes glandulosus Mahnert, 2009	Troglophile	1	Hubei	Mahnert (2009)
Megachernes himalayensis (Ellingsen, 1914)	Troglophile	1	Guangxi	Schawaller (1995)
Megachernes tuberosus Mahnert, 2009	Troglophile	1	Sichuan	Mahnert (2009)
Megachernes vietnamensis Beier, 1967	Troglophile	3	Sichuan, Hubei	Schawaller (1995)
Nudochernes lipase Mahnert, 2003	Troglophile	1	Yunnan	Mahnert (2003)
Nudochernes troglobius Mahnert, 2009	Troglophile	2	Hubei, Sichuan	Mahnert (2009)
Family Chthoniidae				
Lagynochthonius bailongtanensis Li, Liu & Shi, 2019	Troglobiont	1	Yunnan	Li et al. (2019)
Tyrannochthonius akaleus Mahnert, 2009	Troglobiont	1	Sichuan	Mahnert (2009)
Tyrannochthonius antridraconis Mahnert, 2009	Troglobiont	4	Sichuan	Mahnert (2009)
Tyrannochthonius chixingi Gao, Wynne & Zhang, 2018	Troglobiont	1	Guangxi	Gao et al. (2018)
Tyrannochthonius ganshuanensis Mahnert, 2009	Troglobiont	3	Sichuan, Hubei	Mahnert (2009)
Family Neobisiidae				
Bisetocreagris baozinensis Mahnert & Li, 2016	Troglobiont	1	Sichuan	Mahnert and Li (2016)
Bisetocreagris cavernarum Mahnert & Li, 2016	Troglobiont	1	Chongqing	Mahnert and Li (2016)
Bisetocreagris chinacavernicola (Schawaller, 1995)	Troglobiont	2	Sichuan	Schawaller (1995)
Bisetocreagris chuanensis Mahnert & Li, 2016	Troglobiont	2	Guizhou	Mahnert and Li (2016)
Bisetocreagris gracilenta Gao & Zhang, 2017	Troglobiont	1	Guizhou	Gao et al. (2017)
Bisetocreagris guangshanensis Gao & Zhang, 2017	Troglobiont	1	Guizhou	Gao et al. (2017)
Bisetocreagris juanxuae Mahnert & Li, 2016	Troglobiont	1	Sichuan	Mahnert and Li (2016)
Bisetocreagris maomaotou Gao, Wynne & Zhang, 2018	Troglobiont	1	Guangxi	Gao et al. (2018)
Bisetocreagris martii (Mahnert, 2003)	Troglobiont?	1	Yunnan	Mahnert (2003)
Bisetocreagris scaurum (Mahnert, 2003)	Troglobiont	1	Yunnan	Mahnert (2003)
Bisetocreagris titanium (Mahnert, 2003)	Troglobiont	1	Yunnan	Mahnert (2003)
Bisetocreagris xiaoensis Li & Liu, 2017	Troglobiont	1	Yunnan	Li et al. (2017)
Parobisium magangensis Feng, Wynne & Zhang, 2019	Troglobiont	1	Beijing	Feng et al. (2019)
Parobisium motianense sp. nov.	Troglobiont	1	Guizhou	This study
Parobisium qiangzhuang sp. nov.	Troglobiont	1	Guizhou	This study
Parobisium sanlouense sp. nov.	Troglobiont	1	Guizhou	This study
Parobisium tiani sp. nov.	Troglobiont	1	Guizhou	This study
Parobisium yuantongi Feng, Wynne & Zhang, 2019	Troglobiont	1	Beijing	Feng et al. (2019)

Results

Family Neobisiidae Chamberlin, 1930
Subfamily Neobisiinae Chamberlin 1930

Genus *Parobisium* Chamberlin 1930

Neobisium (*Parobisium*) Chamberlin 1930: 17; Beier 1932: 84; Morikawa 1960: 112–113; Hoff 1961: 427.

Parobisium Chamberlin: Chamberlin and Malcolm 1960: 112–113; Chamberlin 1962: 123; Harvey 1991: 394; Mahnert 2003: 744–745.

Type species. *Neobisium* (*Parobisium*) *magnum* Chamberlin, 1930, by original designation.

Key to *Parobisium* species of China

1 Carapace with eyes or eye spots **2**
– Carapace without eyes or eye spots **5**
2 Carapace only with two eyes or eye spots ..... ***P. tiani* sp. nov.**
– Carapace with four eyes or eyespots **3**
3 Eight setae on posterior margin of carapace; pedipalpal femur 4.65 times longer than wide, patella 3.14 times longer than wide..... ***P. xiaowutaicum* Guo & Zhang, 2016**
– Six setae on posterior margin of carapace; both pedipalpal femur and patella more than 5.7 times longer than wide **4**
4 Pedipalp without granulation; pedipalpal femur 8.91–8.97 times longer than wide, patella 7.64–7.84 times longer than wide..... ***P. magangensis* Feng, Wynne & Zhang, 2019**
– Pedipalp with granulation present on femur, inside lateral of patella and chelal hand; pedipalpal femur 6.75 times longer than wide, patella 5.7 times longer than wide ..... ***P. yuantongi* Feng, Wynne & Zhang, 2019**
5 Carapace with four developed eyes; epistome small, triangular; pedipalp without granulation ..... ***P. wangae* Guo & Zhang, 2016**
– Carapace with four eyespots; epistome small, rounded; pedipalp with finely granulation **6**
6 Pedipalpal femur 6.50–6.59 times longer than wide, patella 5.07–5.11 times longer than wide ..... ***P. sanlouense* sp. nov.**
– Boyh pedipalpal femur and patella less than 5.0 times longer than wide..... 7
7 Femur of pedipalp with granulation; pedipalpal femur 3.89–4.11 times longer than wide, patella 2.54–2.60 times longer than wide .... ***P. qiangzhuang* sp. nov.**
– Femur of pedipalp without granulation; pedipalpal femur 4.66–4.9 times longer than wide, patella 3.09–3.39 times longer than wide ..... ***P. motianense* sp. nov.**

***Parobisium motianense* sp. nov.**
http://zoobank.org/D19923FF-CC27-4B00-9A9E-4DB225825490
Figs 2–5

Type material. Holotype male (Ps.-MHBU- GZ17051801): China, Guizhou Province, Pingtang County, Tangbian Town, Motian Cave (Figs 1C, 18), [25°38'32.86"N, 104°46'00.36"E], 869 m elevation, 18 May 2017, Mingyi Tian leg. Paratypes: 2 males (Ps.-MHBU- GZ17051802 & GZ170501803), 1 female (Ps.-MHBU- GZ17051804), same data as for holotype.

Etymology. Latinized adjective derived from the name of the type locality, Motian Cave.

Distribution. This species is known only from the type locality.

Diagnosis. Prior to this study, only four species of *Parobisium* have been reported in China (*Parobisium wangae* Guo & Zhang, 2016, *Parobisium xiaowutaicum* Guo &

Figure 2. *Parobisium motianense* sp. nov. Sex indeterminable from photo.

Zhang, 2016, *Parobisium magangensis* Feng, Wynne & Zhang, 2019 and *Parobisium yuantongi* Feng, Wynne & Zhang, 2019). The new troglomorphic species can be distinguished from other members of the genus *Parobisium* by following combination of characters: carapace with four eye spots on a raised surface (*P. wangae* has four developed eyes, *P. tiani* with two faint eye spots; *P. magangensis*, *P. xiaowutaicum* and *P. yuantongi* lacks eyes/eye spots); epistome small, rounded (small, triangular in *P. wangae*; triangular, with rounded top in *P. tiani* and *P. yuantongi*); carapace with six setae on posterior margin (eight in *P. wangae*; eight in *P. xiaowutaicum*); pedipalpal femur 4.66–4.90 times longer than wide (8.91–8.97 times in *P. magangensis*; 3.89–4.11 times in *P. qiangzhuang*; 6.50–6.59 times in *P. sanlouense*; 5.63–5.73 times in *P. tiani*; 3.60–3.65 times in *P. wangae*; 6.75 times in *P. yuantongi*); patella 3.09–3.39 times longer than wide (7.64–7.84 times in *P. magangensis*; 2.54–2.60 times in *P. qiangzhuang*; 5.07–5.11 times in *P. sanlouense*; 4.52–4.58 times in *P. tiani*; 1.89–2.16 times in *P. wangae*; 5.70 times in *P. yuantongi*;); pedipalpal hand which is finely granular (smooth in *P. magangensis*, *P. wangae* and *P. xiaowutaicum*; with granulation present on inside lateral of femur and chelal hand in *P. qiangzhuang* and *P. sanlouense*; with granulation present on femur, inside lateral of patella and chelal hand in *P. yuantongi*); chela (with pedicel) 3.72–4.06 times longer than wide (8.67–8.69 times in *P. magangensis*; 3.12–3.25 times in *P. qiangzhuang*; 6.08–6.34 times in *P. sanlouense*; 4.97–5.03 times in *P. tiani*; 3.13–3.52 times in *P. wangae*; 3.14 times in *P. xiaowutaicum*; 5.70 times in *P. yuantongi*); both chelal finger has 95–98 teeth (146–162 in *P. magangensis*; 69–80 in

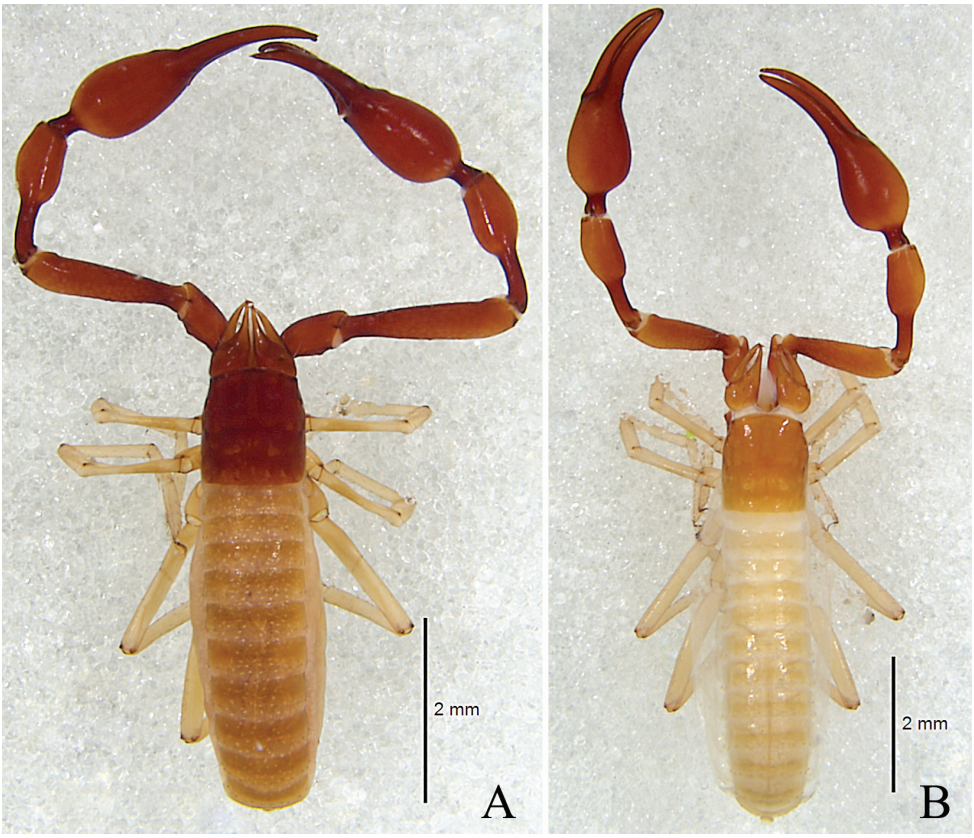

Figure 3. *Parobisium motianense* sp. nov. **A** Holotype male, dorsal view **B** Paratype female, dorsal view.

P. qiangzhuang; 119–130 in *P. sanlouensis*; 57–74 in *P. wangae*; 73–75 in *P. xiaowutaicum*; 116–118 in *P. yuantongi*).

Description. Male (Fig. 3A). Carapace, chelicerae, and pedipalps yellowish brown to reddish brown; abdomen and legs yellowish.

Carapace (Figs 4A, 5A): Smooth, 1.16–1.20 times longer than broad, with a total of 28–30 setae, including 4 on anterior margin, 6 on posterior margin, and 1 on each side of anterior lateral margin; with four eye spots on a raised surface (Fig. 4B); epistome small, rounded.

Chelicera (Figs 4C, 5B): Hand with 7 setae, movable finger with 1 submedial seta; fixed finger with 12–14 teeth; movable finger with 14–15 teeth; serrula exterior with 40–44 lamellae; serrula interior with 25–29 lamellae. Galea (Fig. 5E) replaced by a small rounded transparent sclerotic knob. Rallum (Fig. 5C) with 8 pinnate blade, distal-most blade with expanded base, and together with the second blade slightly separated from the others, proximal one short.

Pedipalps (Figs 4D–E, 5H–J): Apex of coxa rounded, with 5 setae on each side, pedipalpal coxa with 7 setae. Pedipalp smooth and slender except for hand, which is

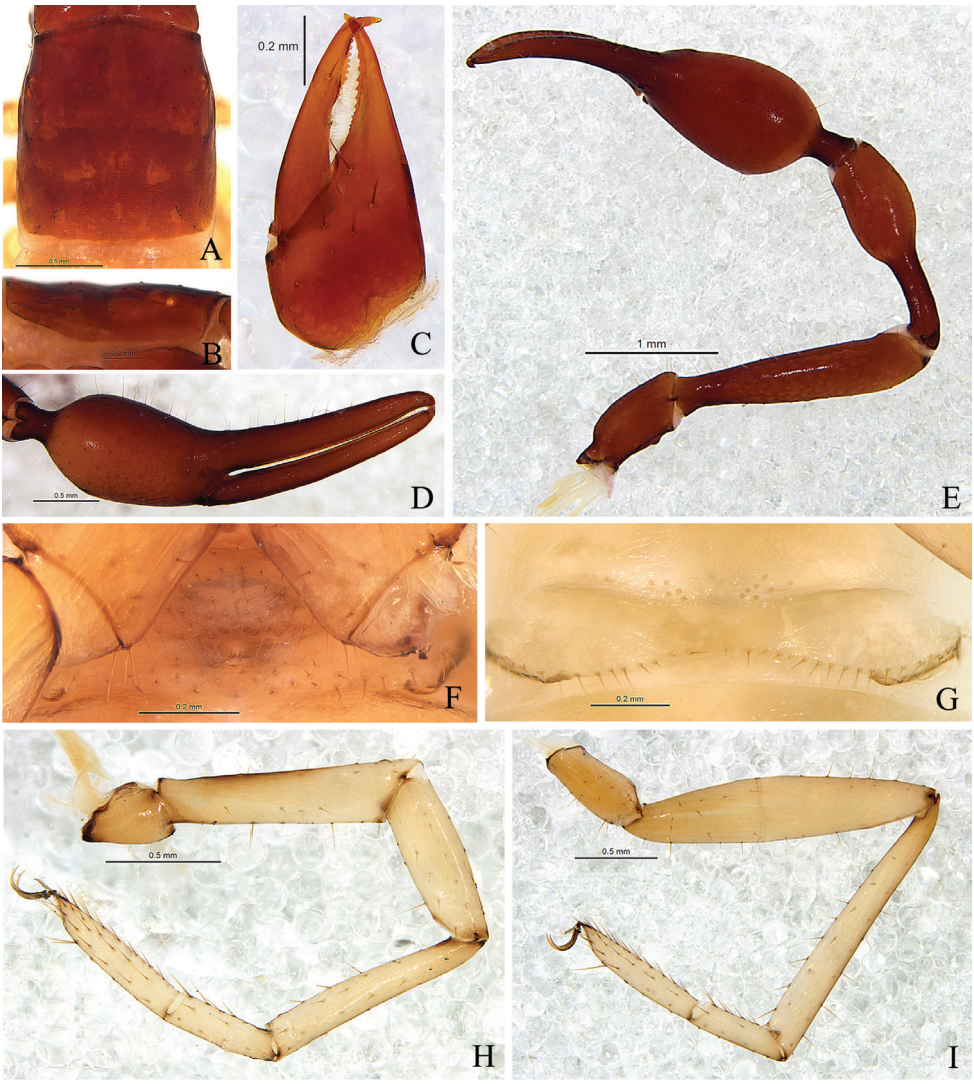

Figure 4. *Parobisium motianense* sp. nov., holotype male (**A**–**F**, **H**–**I**), female (**G**). **A** Carapace, dorsal view **B** Eye area, lateral view **C** Left chelicera, dorsal view **D** Right chela, lateral view **E** Right pedipalp, dorsal view **F** Male genitalia **G** Female genitalia **H** Left leg I, lateral view **I** Left leg IV, lateral view.

finely granular. Trochanter 2.04–2.22 times longer than wide, femur 4.66–4.90, patella 3.09–3.39 times longer than wide, pedicel about half the entire length of patella, chela (with pedicel) 3.72–4.06, chela (without pedicel) 3.35–3.71 times longer than wide, movable finger 1.43–1.45 times longer than hand (without pedicel). Fixed chelal finger with 8 trichobothria, movable finger with 4, *eb* and *esb* on lateral margin of hand; *ib*, *ist*, and *isb* closely grouped at the base of the fixed finger; *est* slightly distal of finger middle; *it* closer to fingertip than *et*; on movable finger, *st* nearer to *t* than to *sb*, the distance between *sb* and *b* is somewhat equal to that of *sb* and *st* (Figs 4D, 5H–I). Venom apparatus present only in fixed chelal finger, venom duct short, not extending

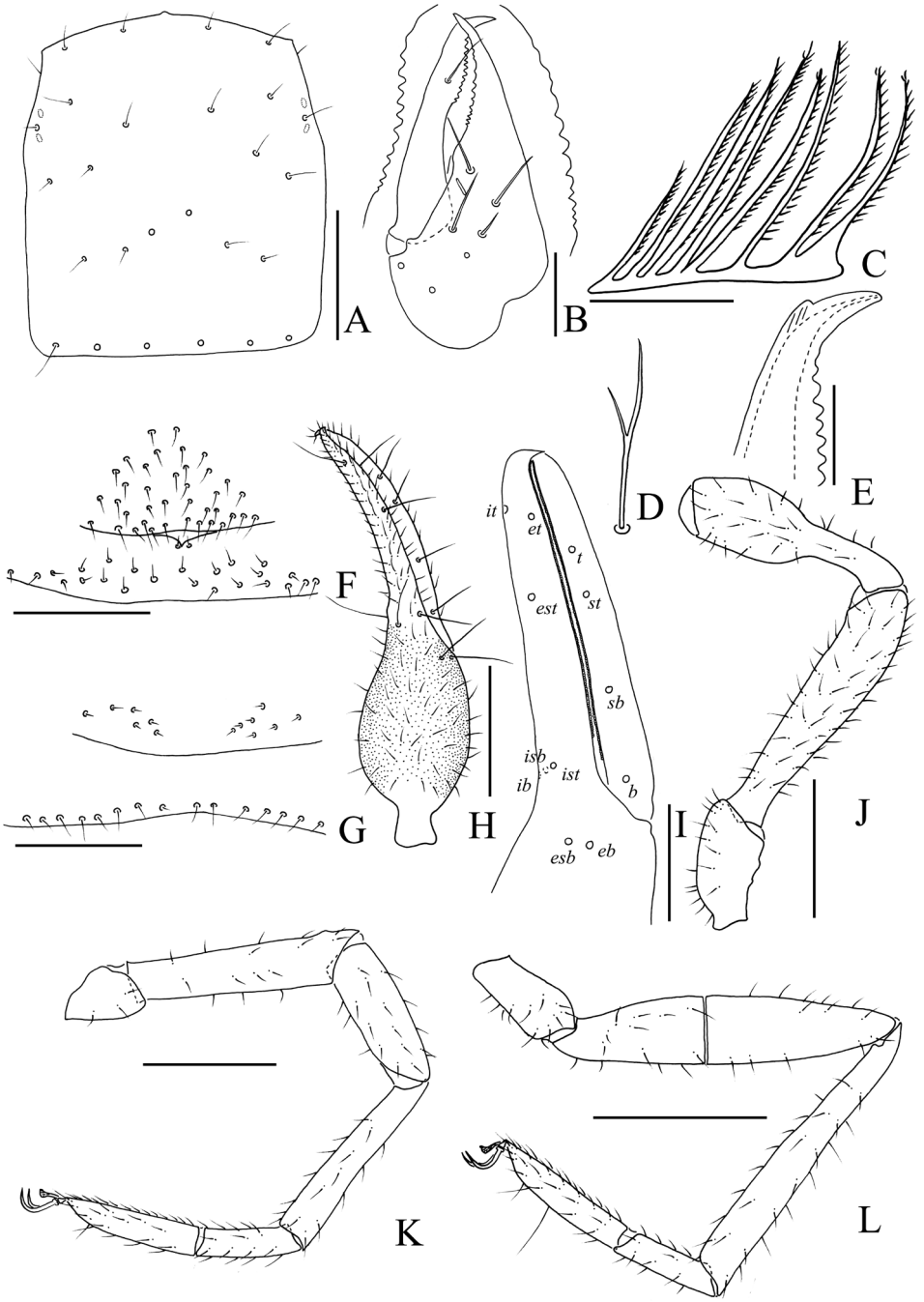

Figure 5. *Parobisium motianense* sp. nov., holotype male (**A**–**F**, **H**–**L**), female (**G**). **A** Carapace, dorsal view **B** Left chelicera, dorsal view **C** Rallum **D** Subterminal tarsal seta **E** Movable finger of chelicera, showing sclerotic knob **F** Male genitalia **G** Female genitalia **H** Right chela, dorsal view **I** Right chelal fingers, lateral view **J** Right pedipalp, dorsal view (trochanter, femur, and patella) **K** Left leg I, lateral view **L** Left leg IV, lateral view. Scale bars: 0.1 mm (**C**, **D**–**E**), 0.25 mm (**B**, **F**–**G**), 0.5 mm (**A**, **I**), 1 mm (**H**, **J**–**L**).

beyond half the distance to *et*. Fixed chelal finger with 96–98 teeth, movable finger with 95–97 teeth.

Abdomen: Pleural membrane granulated. Tergal chaetotaxy (I–XI): 8–11/9–10/9/9–11/10–11/10–11/9–12/11–12/11–12/10–11/6–8; sternal chaetotaxy (IV–XI): 9–10/14–16/15–16/15/13–16/12–14/12–15/2; stigmata with 5–6 setae; anal cone with 2 dorsal and 2 ventral setae. Male genital area (Figs 4F, 5F): sternite II with 35–38 scattered setae; sternite III with anteromedian groove flanked by one small seta on each side, with 20–26 posterior setae.

Legs: Coxa chaetotaxy (I–IV): 8–9/6–7/3–4/9–10. Leg I (Figs 4H, 5K): femur 4.37–4.96, patella 2.92–3.22, tibia 6.00–7.27, basitarsus 3.33–3.85, telotarsus 5.50–5.57 times longer than deep, femur 1.55–1.61 times longer than patella, telotarsus 1.54–1.56 times longer than basitarsus. Leg IV (Figs 4I, 5L): femur + patella 4.36–5.00 times longer than deep, femur shorter than patella; tibia 8.04–9.05, basitarsus 3.81–3.88, telotarsus 5.44–6.36 times longer than deep, telotarsus 1.35–1.43 times longer than basitarsus; tibia with one tactile setae (TS=0.52–0.54), basitarsus with one tactile setae (TS=0.15–0.16), telotarsus with one tactile setae (TS=0.49–0.53); subterminal tarsal seta (Fig. 5D) bifurcate; arolium not divided, shorter than the slender and simple claws.

Female (paratype; Fig. 3B): Mostly same as holotype.

Chelicera. Hand with 7 setae, movable finger with 1 submedial seta; fixed finger with 15–17 teeth; movable finger with 14–15 teeth; serrula exterior with 41 lamellae; serrula interior with 23 lamellae. Galea replaced by a conspicuous semicircular transparent sclerotic knob; rallum of 8 blades, similar to holotype.

Pedipalps. Pedipalpal coxa with 8–9 setae. Trochanter 2.08, femur 4.52, patella 3.02, chela (with pedicel) 3.69, chela (without pedicel) 3.33 times longer than wide, movable finger 1.22 times longer than hand (without pedicel). Fixed chelal finger with 97 teeth, movable finger with 95 teeth.

Abdomen. Tergal chaetotaxy (I–XI): 8/7/9/10/10/11/11/11/11/10/6; sternal chaetotaxy (IV–XI): 11/16/17/16/16/14/12/2. Female genital area (Figs 4G, 5G): sternite II with 6–7 setae on each side; sternite III with a row of 20 setae on the posterior margin.

Measurements: (length/breadth or depth in mm; ratios for most characters in parentheses). Male (holotype and paratypes). Body length 4.26–4.78. Carapace 1.16–1.20 (1.31–1.36/1.13). Pedipalpal trochanter 2.04–2.22 (0.91–0.96/0.41–0.47), femur 4.66–4.90 (1.96–2.05/0.40–0.44), patella 3.09–3.39 (1.66–1.73/0.49–0.56), chela (with pedicel) 3.72–4.06 (3.09–3.13/0.77–0.83), chela (without pedicel) 3.35–3.71 (2.78–2.86/0.77–0.83), hand length (without pedicel) 1.30–1.31, movable finger length 1.86–1.90 (1.43–1.45 times longer than hand without pedicel). Leg I: trochanter 1.36–1.50 (0.39/0.26–0.28), femur 4.37–4.96 (1.18–1.19/0.24–0.27), patella 2.92–3.22 (0.74–0.76/0.23–0.26), tibia 6.00–7.27 (1.02–1.09/0.15–0.17), basitarsus 3.33–3.85 (0.50/0.13–0.15), telotarsus 5.57–5.50 (0.77–0.78/0.14). Leg IV: trochanter 2.13–2.44 (0.64–0.67/0.27–0.30), femur + patella 4.36–5.00 (1.90–1.92/0.38–0.44), tibia 8.04–9.05 (1.85–1.90/0.21–0.23), basitarsus 3.81–3.88 (0.61–0.66/0.16–17), telotarsus 5.44–6.36 (0.87–0.89/0.14–0.16).

Female (paratype). Body length 5.99. Carapace 1.14 (1.46/1.28). Pedipalpal trochanter 2.08 (1.02/0.49), femur 4.52 (2.08/0.46), patella 3.02 (1.81/0.60), chela (with pedicel) 3.69 (3.28/0.89), chela (without pedicel) 3.33 (2.96/0.89), hand length (without pedicel) 1.47, movable finger length 1.79 (1.22 times longer than hand without pedicel). Leg I: trochanter 1.47 (0.44/0.30), femur 4.62 (1.20/0.26), patella 3.57 (0.82/0.23), tibia 6.76 (1.15/0.17), basitarsus 3.40 (0.51/0.15), telotarsus 5.13 (0.77/0.15). Leg IV: trochanter 2.28 (0.73/0.32), femur + patella 5.10 (1.99/0.39), tibia 8.58 (2.06/0.24), basitarsus 3.72 (0.67/0.18), telotarsus 5.29 (0.90/0.17).

***Parobisium qiangzhuang* sp. nov.**

http://zoobank.org/F122663A-2AF0-437C-83C5-791E9739854C

Figs 6–9

Type material. Holotype male (Ps.-MHBU- GZ19080301): China, Guizhou Province, Anshun City, Ziyun County, Daying Town, Zharou Cave (Figs 1B, 19), [25°29'24.87"N, 106°18'28.65"E], estimated cave deep zone, 1139 m elevation, 3 August 2019, Zegang Feng, Chen Zhang leg. Paratypes: 2 Males (Ps.-MHBU-GZ19080302- GZ19080303), same data as for holotype; 1 Female (Ps.-MHBU-GZ19061201), same location as holotype, 12 June 2018, Sunbin Huang, Zhuanghui Qin, Mengzhen Chen, Lei Tao leg.

Etymology. The species name, *qiangzhuang*, was derived from the Latinized Mandarin phrase for "strong and hardy" qiáng zhuàng (强壮), which refers to the shape of chela.

Distribution. Species known only from the type locality.

Diagnosis. The subterranean-adapted *Parobisium qiangzhuang* can be distinguished from other members of the genus *Parobisium* by following combination of characters: carapace with four eye spots on a raised surface (*P. wangae* has four developed eyes, *P. tiani* with two faint eye spots; *P. magangensis*, *P. xiaowutaicum* and *P. yuantongi* lacks eyes/eye spots); epistome small, rounded (small, triangular in *P. wangae*; triangular, with rounded top in *P. tiani* and *P. yuantongi*); pedipalpal femur 3.89–4.11 times longer than wide (8.91–8.97 times in *P. magangensis*; 4.66–4.90 times in *P. motianense*; 6.50–6.59 times in *P. sanlouense*; 5.63–5.73 times in *P. tiani*; 4.65 times in *P. xiaowutaicum*; 6.75 times in *P. yuantongi*); patella 2.54–2.60 times longer than wide (7.64–7.84 times in *P. magangensis*; 3.09–3.39 times in *P. motianense*; 5.07–5.11 times in *P. sanlouense*; 4.52–4.58 times in *P. tiani*; 3.14 times in *P. xiaowutaicum*; 5.70 times in *P. yuantongi*;); pedipalpal hand and inside lateral of femur, which is finely granular (smooth in *P. magangensis*, *P. wangae* and *P. xiaowutaicum*; with granulation present on chelal hand in *P. tiani*; with granulation present on femur, inside lateral of patella and chelal hand in *P. yuantongi*); chela (with pedicel) 3.12–3.52 times longer than wide (8.67–8.69 times in *P. magangensis*; 3.72–4.06 times in *P. motianense*; 6.08–6.34 times in *P. qiangzhuang*; 4.97–5.03 times in *P. tiani*; 5.70 times in *P. yuantongi*); both chelal finger has 69–80 teeth (146–162 in *P. magangensis*; 96–98 in *P. motianense*; 119–130 in *P. sanlouensis*; 104–112 in *P. tiani*; 116–118 in *P. yuantongi*).

Figure 6. *Parobisium qiangzhuang* sp. nov. Male habitus.

Description. Male (Fig. 7A). Carapace, chelicerae, and pedipalps reddish brown; abdomen and legs yellowish.

Carapace (Figs 8A, 9A): Smooth, 1.15–1.24 times longer than broad, with a total of 28–31 setae, including 4 on anterior margin, 6–8 on posterior margin, and 1–2 on each side of anterior lateral margin; with 4 eye spots on a raised surface (Fig. 8B); epistome small and rounded.

Chelicera (Figs 8C, 9B): Hand with 7 setae, movable finger with 1 submedial seta; fixed finger with 9–11 teeth; movable finger with 10–13 teeth; serrula exterior with 34–38 lamellae; serrula interior with 20–24 lamellae. Galea (Fig. 9D) replaced by a small rounded transparent sclerotic knob. Rallum (Fig. 9C) with 8 pinnate blade, distal-most blade with expanded base, proximal one short.

Pedipalps (Figs 8D–E, 9H–J): Apex of coxa rounded, with 5 setae on each side, pedipalpal coxa with 9 setae. Pedipalp smooth except for hand and inside lateral of femur, which is finely granular. Trochanter 1.84–1.97 times longer than wide, femur 3.89–4.11, patella 2.54–2.60 times longer than wide, pedicel about half the entire length of patella, chela (with pedicel) 3.12–3.25, chela (without pedicel) 2.86–2.97 times longer than wide, movable finger 1.11–1.15 times longer than hand (without pedicel). Fixed chelal finger with 8 trichobothria, movable finger with 4, *eb* and *esb* on lateral margin of hand; *ib*, *ist* and *isb* closely grouped at the base of the fixed finger; *est* slightly distal of finger middle; *it-et* at same level near fingertip; on movable finger *st* nearer to *t* than to *sb*, the distance between *sb* and *b* is somewhat equal to that of *sb* and *st* (Figs 8D, 9H–I). Venom apparatus present only in fixed chelal finger, venom

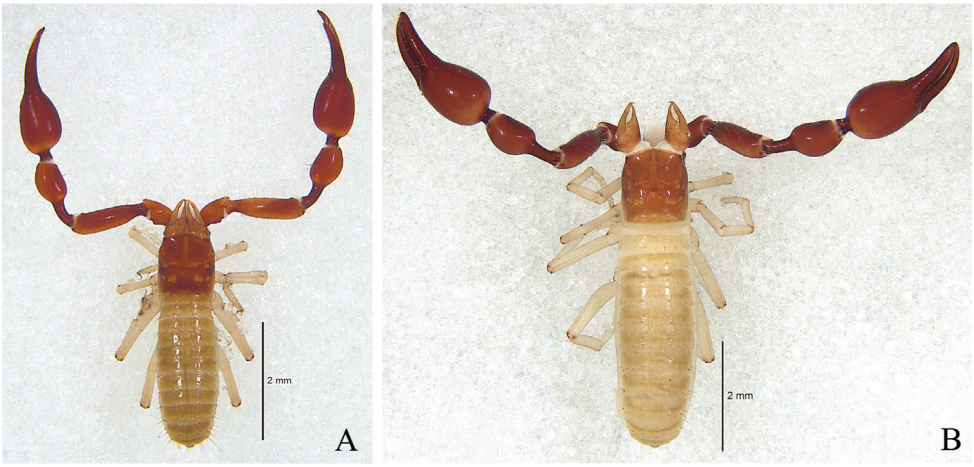

Figure 7. *Parobisium qiangzhuang* sp. nov. **A** Holotype male, dorsal view **B** Paratype female, dorsal view.

duct short, not extending past half of the distance to *et*. Fixed chelal finger with 71–75 teeth, movable finger with 69–80 teeth.

Abdomen: Pleural membrane granulated. Tergal chaetotaxy (I–XI): 10–11/11/11–12/12/12–13/12/12/12/12/12–13/12/7–9; sternal chaetotaxy (IV–XI): 9–11/13–15/14–16/13–16/13–15/12–14/12–15/3–4; stigmata with 4–5 setae; anal cone with 2 dorsal and 2 ventral setae. Male genital area (Figs 8F, 9E): sternite II with 28–30 scattered setae; sternite III with anteromedian groove flanked by one small seta on each side, with 17–19 posterior setae.

Legs: Coxa chaetotaxy (I–IV): 9–11/7–10/4–5/9–11. Leg I (Figs 8H, 9K): femur 3.52–3.55, patella 2.89–2.94, tibia 5.85–6.67, basitarsus 2.67–2.82, telotarsus 4.42–4.82 times longer than deep, femur 1.40–4.42 times longer than patella, telotarsus 1.66–1.71 times longer than basitarsus. Leg IV (Figs 8I, 9L): femur + patella 3.63–3.65 times longer than deep, femur shorter than patella, tibia 6.45–6.79, basitarsus 2.93, telotarsus 4.40–4.57 times longer than deep, telotarsus 1.50–1.56 times longer than basitarsus; tibia with one tactile setae (TS=0.48–0.50), basitarsus with one tactile setae (TS=0.11–0.15), telotarsus with one tactile setae (TS=0.41–0.45); subterminal tarsal seta (Fig. 9G) bifurcate, both branches dentate; arolium not divided, shorter than the slender and simple claws.

Female (paratype) (Fig. 7B): Mostly same as holotype.

Chelicera. Hand with 7 setae, movable finger with 1 submedial seta; fixed finger with 13 teeth; movable finger with 12 teeth; serrula exterior with 38 lamellae; serrula interior with 24 lamellae. Galea replaced by conspicuous semicircular transparent sclerotic knob; rallum of 8 blades, but similar to holotype.

Pedipalps. Pedipalpal coxa with 10–11 setae. Trochanter 2.02, femur 3.60, patella 2.18, chela (with pedicel) 2.86, chela (without pedicel) 2.63 times longer than wide, movable finger 1.01 times longer than hand (without pedicel). Fixed chelal finger with about 72 teeth, movable finger with about 78 teeth.

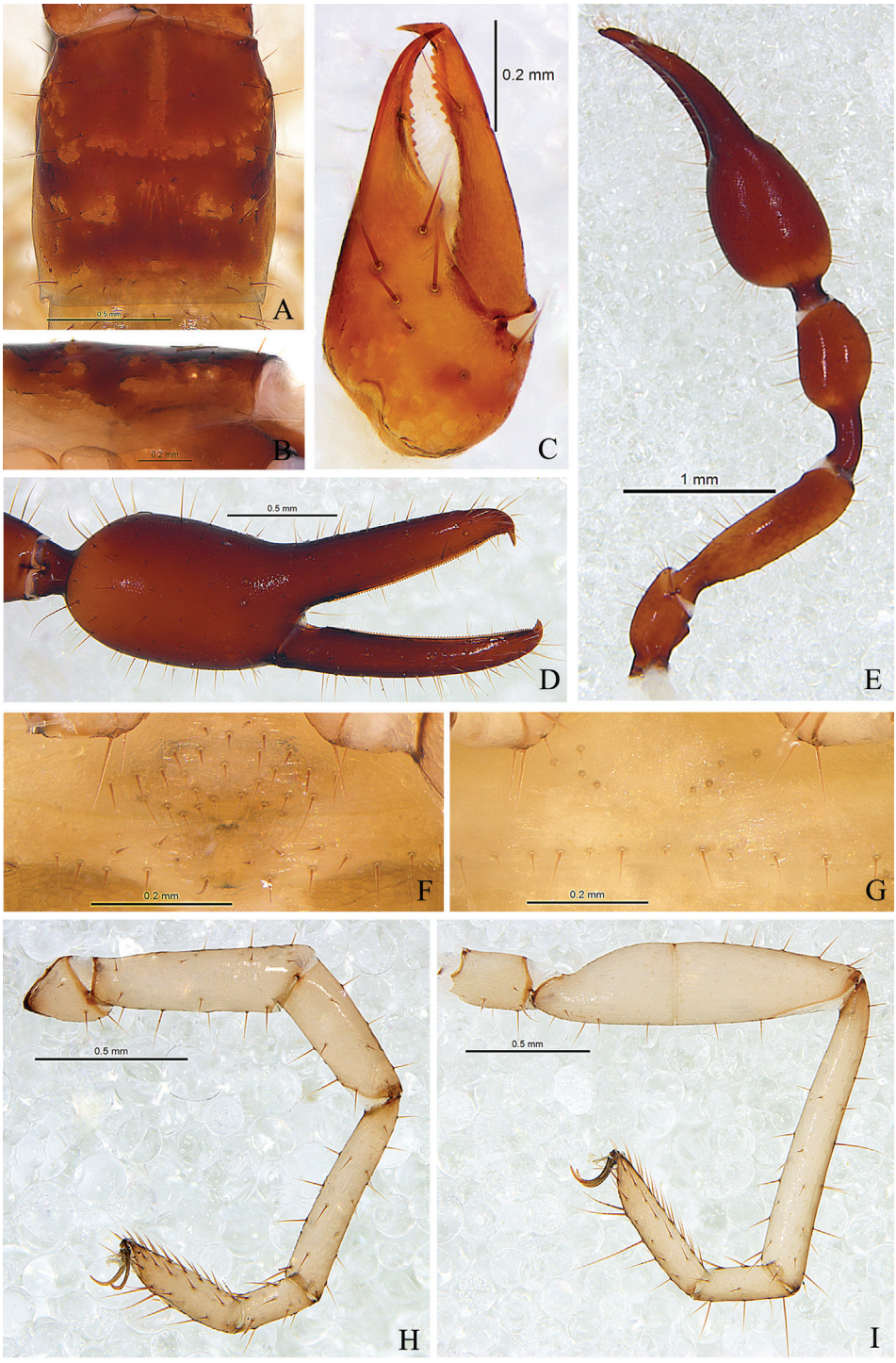

Figure 8. *Parobisium qiangzhuang* sp. nov. holotype male (**A**–**F**, **H**–**I**), female (**G**): **A** Carapace, dorsal view **B** Eye area, lateral view **C** Right chelicera, dorsal view **D** Right chela, lateral view **E** Right pedipalp, dorsal view **F** Male genitalia **G** Female genitalia **H** Right leg I, lateral view **I** Right leg IV, lateral view.

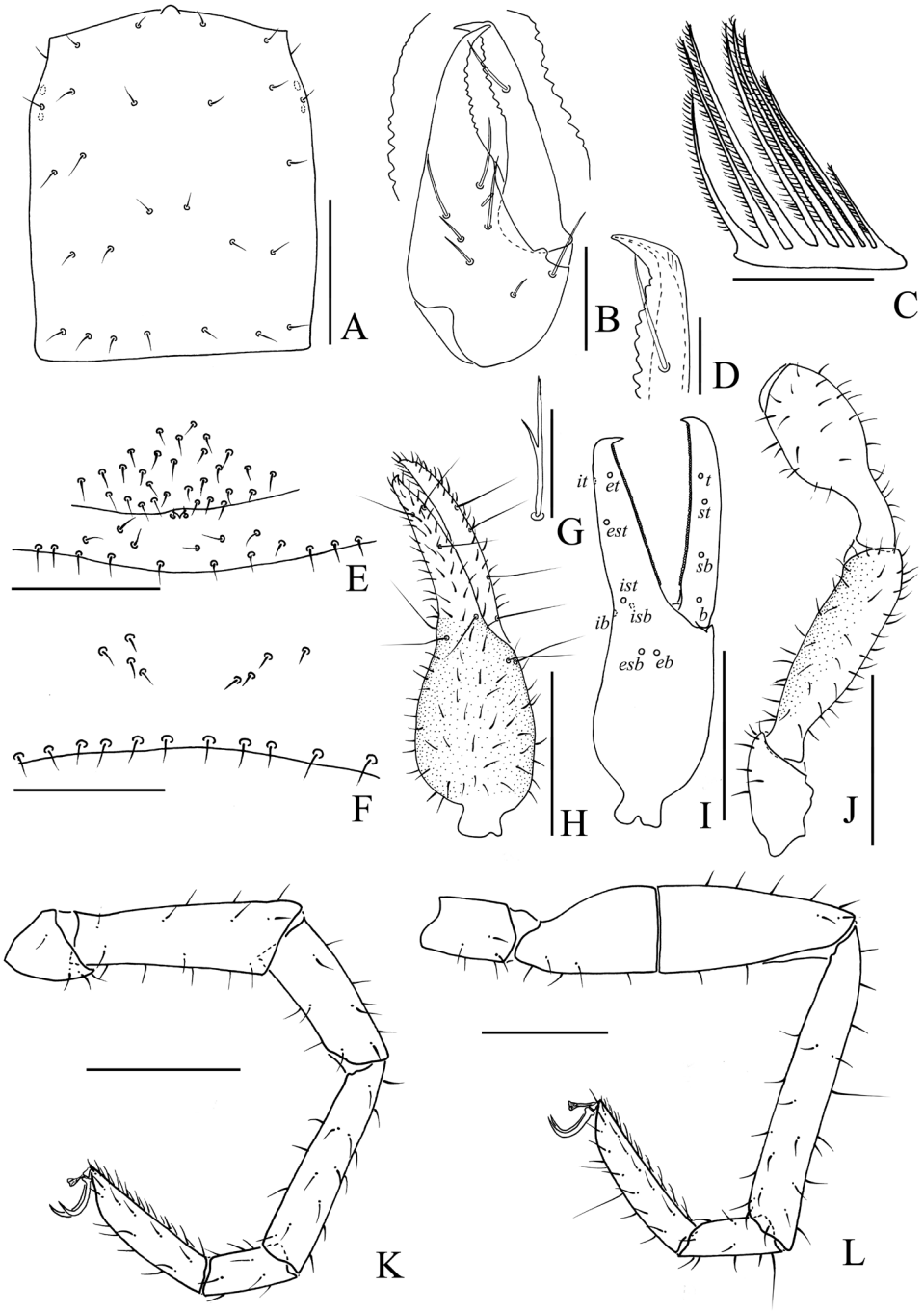

Figure 9. *Parobisium qiangzhuang* sp. nov., holotype male (**A**–**E**, **G**–**L**), female (**F**). **A** Carapace, dorsal view **B** Right chelicera, dorsal view **C** Rallum **D** Movable finger of chelicera, showing sclerotic knob **E** Male genitalia **F** Female genitalia **G** Subterminal tarsal seta **H** Right chela, dorsal view **I** Right chelal fingers, lateral view **J** Right pedipalp, dorsal view (trochanter, femur, and patella) **K** Right leg I, lateral view **L** Right leg IV, lateral view. Scale bars: 0.1 mm (**C**–**D**, **G**), 0.25 mm (**B**, **E**–**F**), 0.5 mm (**A**, **K**–**L**), 1 mm (**H**–**J**).

Abdomen. Tergal chaetotaxy (I–XI): 8/11/13/13/12/12/13/13/13/12/5; sternal chaetotaxy (IV–XI): 7/16/14/14/15/14/12/5. Female genital area (Figs 8G, 9F): sternite II with 4 setae on each side; sternite III with a row of 12 setae on the posterior margin.

Measurements: (length/breadth or depth in mm; ratios for most characters in parentheses). Male (holotype and paratypes). Body length 3.61–4.42. Carapace 1.15–1.24 (1.12–1.18/0.95–0.97). Pedipalpal trochanter 1.84–1.97 (0.70–0.75/0.38), femur 3.89–4.11 (1.40–1.48/0.36), patella 2.54–2.60 (1.22–1.30/0.48–0.50), chela (with pedicel) 3.12–3.25 (2.18–2.28/0.67–0.73), chela (without pedicel) 2.86–2.97 (1.99–2.09/0.67–0.73), hand length (without pedicel) 1.02–1.11, movable finger length 1.17–1.23 (1.11–1.15 times longer than hand without pedicel). Leg I: trochanter 1.17–1.30 (0.27–0.30/0.23), femur 3.52–3.55 (0.74–0.78/0.21–0.22), patella 2.89–2.94 (0.53–0.55/0.18–0.19), tibia 5.85–6.67 (0.76–0.80/0.12–0.13), basitarsus 2.67–2.82 (0.31–0.32/0.11–0.12), telotarsus 4.42–4.82 (0.53/0.11–0.12). Leg IV: trochanter 2.08–2.30 (0.50–0.53/0.23–0.24), femur + patella 3.63–3.65 (1.24–1.27/0.34–0.35), tibia 2.93 (0.41–0.44/0.14–0.15), basitarsus 3.81–3.88 (0.61–0.66/0.16–17), telotarsus 4.40–4.57 (0.64–0.66/0.14–0.15).

Female (paratype). Body length 5.49. Carapace 1.24 (1.50/1.21). Pedipalpal trochanter 2.02 (0.91/0.45), femur 3.60 (1.69/0.47), patella 2.18 (1.46/0.67), chela (with pedicel) 2.86 (2.69/0.94), chela (without pedicel) 2.63 (2.47/0.94), hand length (without pedicel) 1.37, movable finger length 1.38 (1.01 times longer than hand without pedicel). Leg I: trochanter 1.26 (0.34/0.27), femur 3.54 (0.85/0.24), patella 2.86 (0.63/0.22), tibia 7.08 (0.92/0.13), basitarsus 3.17 (0.38/0.12), telotarsus 4.46 (0.58/0.13). Leg IV: trochanter 2.07 (0.60/0.29), femur + patella 4.11 (1.56/0.38), tibia 7.55 (1.51/0.20), basitarsus 2.81 (0.45/0.16), telotarsus 4.67 (0.70/0.15).

Parobisium sanlouense sp. nov.

http://zoobank.org/EC06FD6A-41EB-47A5-A31A-BC2EC89941A7

Figs 10–13

Type material. Holotype male (Ps.-MHBU-GZ15050201): China, Guizhou Province, Fuquan County, Sanlou Cave (Figs 1D, 20), [26°56'46"N, 107°18'47"E], 1280 m elevation, 02 May 2015, Mingyi Tian leg. Paratypes: 3 males (Ps.-MHBU-GZ19072901, GZ19072902, GZ19072903), 3 females (Ps.-MHBU- GZ19072904, GZ19072905, GZ19072906), same location as holotype, estimated cave deep zone, 29 July 2019, Zegang Feng, Chen Zhang, Zhaoyi Li, Yonghao Li leg.

Etymology. Latinized adjective derived from the name of the type locality, Sanlou Cave.

Distribution. This species is known only from the type locality.

Diagnosis. This new species can be easily distinguished from other members of the genus *Parobisium* by following combination of characters: carapace with four eye spots on a slightly raised (*P. wangae* has four developed eyes, *P. tiani* with two faint eye spots; *P. magangensis*, *P. xiaowutaicum* and *P. yuantongi* lacks eyes/eye spots); epistome small, rounded (small, triangular in *P. wangae*; triangular, with rounded top in *P. tiani* and *P. yuantongi*); pedipalpal femur 6.50–6.59 times longer than wide (8.91–8.97 times in

Figure 10. *Parobisium sanlouense* sp. nov. Male habitus.

P. magangensis; 4.66–4.90 times in *P. motianense*; 3.89–4.11 times in *P. qiangzhuang*; 5.63–5.73 times in *P. tiani*; 3.60–3.65 times in *P. wangae*; 4.65 times in *P. xiaowutaicum*); patella 5.07–5.11 times longer than wide (7.64–7.84 times in *P. magangensis*; 3.09–3.39 times in *P. motianense*; 2.54–2.60 times in *P. qiangzhuang*; 4.52–4.58 times in *P. tiani*; 1.89–2.16 times in *P. wangae*; 3.14 times in *P. xiaowutaicum*; 5.70 times in *P. yuantongi*;); pedipalpal hand and inside lateral of femur, which is finely granular (smooth in *P. magangensis*, *P. wangae* and *P. xiaowutaicum*; with granulation present on chelal hand in *P. tiani*; with granulation present on femur, inside lateral of patella and chelal hand in *P. yuantongi*); chela (with pedicel) 6.08–6.34 times longer than wide (8.67–8.69 times in *P. magangensis*; 3.72–4.06 times in *P. motianense*; 3.12–3.25 times in *P. qiangzhuang*; 4.97–5.03 times in *P. tiani*; 3.13–3.52 times in *P. wangae*; 3.14 times in *P. xiaowutaicum*; 5.70 times in *P. yuantongi*); both chelal finger has 119–130 teeth (146–162 in *P. magangensis*; 95–98 in *P. motianense*; 69–80 in *P. qiangzhuang*; 57–74 in *P. wangae*; 73–75 in *P. xiaowutaicum*).

Description. Male (Fig. 11A). Carapace, chelicerae, and pedipalps reddish brown or yellowish brown; abdomen and legs yellowish.

Carapace (Figs 12A, 13A): Smooth, 1.21–1.30 times longer than broad, with a total of 29–31 setae, including 4 on anterior margin, 7 on posterior margin, and 1–2 on each side of anterior lateral margin; with 4 eye spots on a slightly raised surface (Fig. 12B); epistome small, rounded.

Chelicera (Figs 12C, 13B): Hand with 7 setae, movable finger with 1 submedial seta; fixed finger with 13–14 teeth; movable finger with 13–15 teeth; serrula exterior with 39–40 lamellae; serrula interior with 25–27 lamellae. Galea (Fig. 13F) replaced

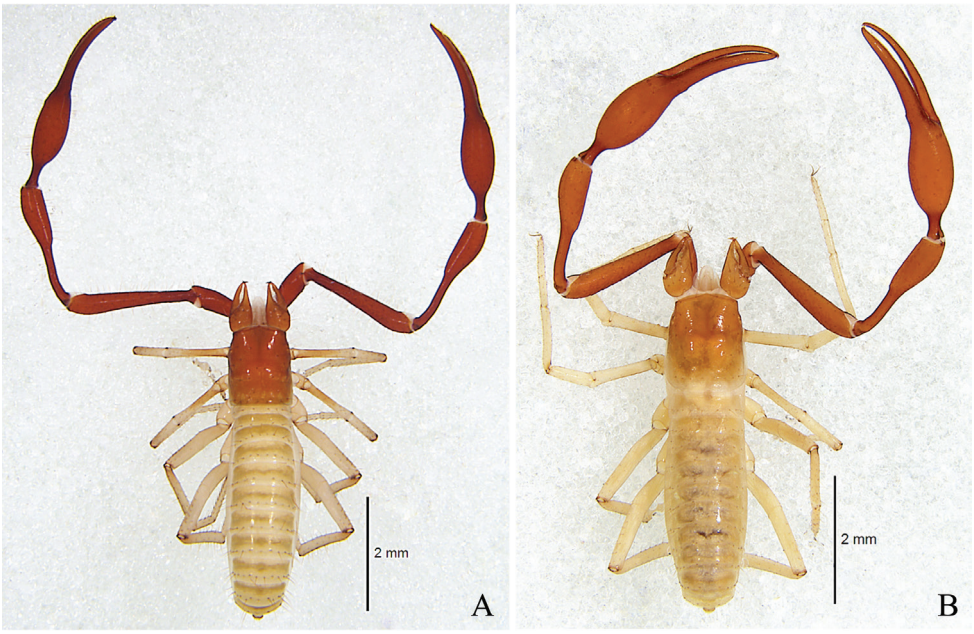

Figure 11. *Parobisium sanlouense* sp. nov. **A** Holotype male, dorsal view **B** Paratype female, dorsal view.

by a small rounded transparent sclerotic knob. Rallum (Fig. 13C) with 8 pinnate blade, distal-most blade with expanded base, proximal one short.

Pedipalps (Figs 12D–E, 13H, J–K): Apex of coxa rounded, with 5 setae on each side, pedipalpal coxa with 8–10 setae. Pedipalp smooth and slender except for hand and inside lateral of femur, which is finely granular. Trochanter 2.86–2.92 times longer than wide, femur 6.50–6.59, patella 5.07–5.11 times longer than wide, pedicel about half the entire length of patella, chela (with pedicel) 6.08–6.34, chela (without pedicel) 5.44–5.62 times longer than wide, movable finger 1.51–1.57 times longer than hand (without pedicel). Fixed chelal finger with 8 trichobothria, movable finger with 4, *eb* and *esb* on lateral margin of hand; *ib*, *ist* and *isb* closely grouped at the base of the fixed finger; *est* slightly distal of finger at middle; *it* slightly closer to fingertip than *et*; on movable finger *st* nearer to *t* than to *sb*, the latter slightly nearer *b* than to *st* (Figs 12D, 13H, J). Venom apparatus present only in fixed chelal finger, venom duct short, not extending past half of the distance to *et*. Fixed chelal finger with 126–130 teeth, movable finger with 119–126 teeth.

Abdomen: Pleural membrane granulated. Tergal chaetotaxy (I–XI): 7/7–9/9–10/10/8–10/11/11/11/11–12/11/7; sternal chaetotaxy (IV–XI): 9–10/13/12/12–13/10–13/13–14/12/3; stigmata with 4–6 setae; anal cone with 2 dorsal and 2 ventral setae. Male genital area (Figs 12F, 13D): sternite II with 34–36 scattered setae; sternite III with anteromedian groove flanked by one small seta on each side, with 21–30 posterior setae.

Legs: Coxa chaetotaxy (I–IV): 8–9/5–6/5/9. Leg I (Figs 12H, 13L): femur 5.08–5.73, patella 3.82–4.05, tibia 8.21–8.57, basitarsus 4.00–4.33, telotarsus 6.08–6.58 times longer than deep, femur 1.45–1.48 times longer than patella, telotarsus 1.40–

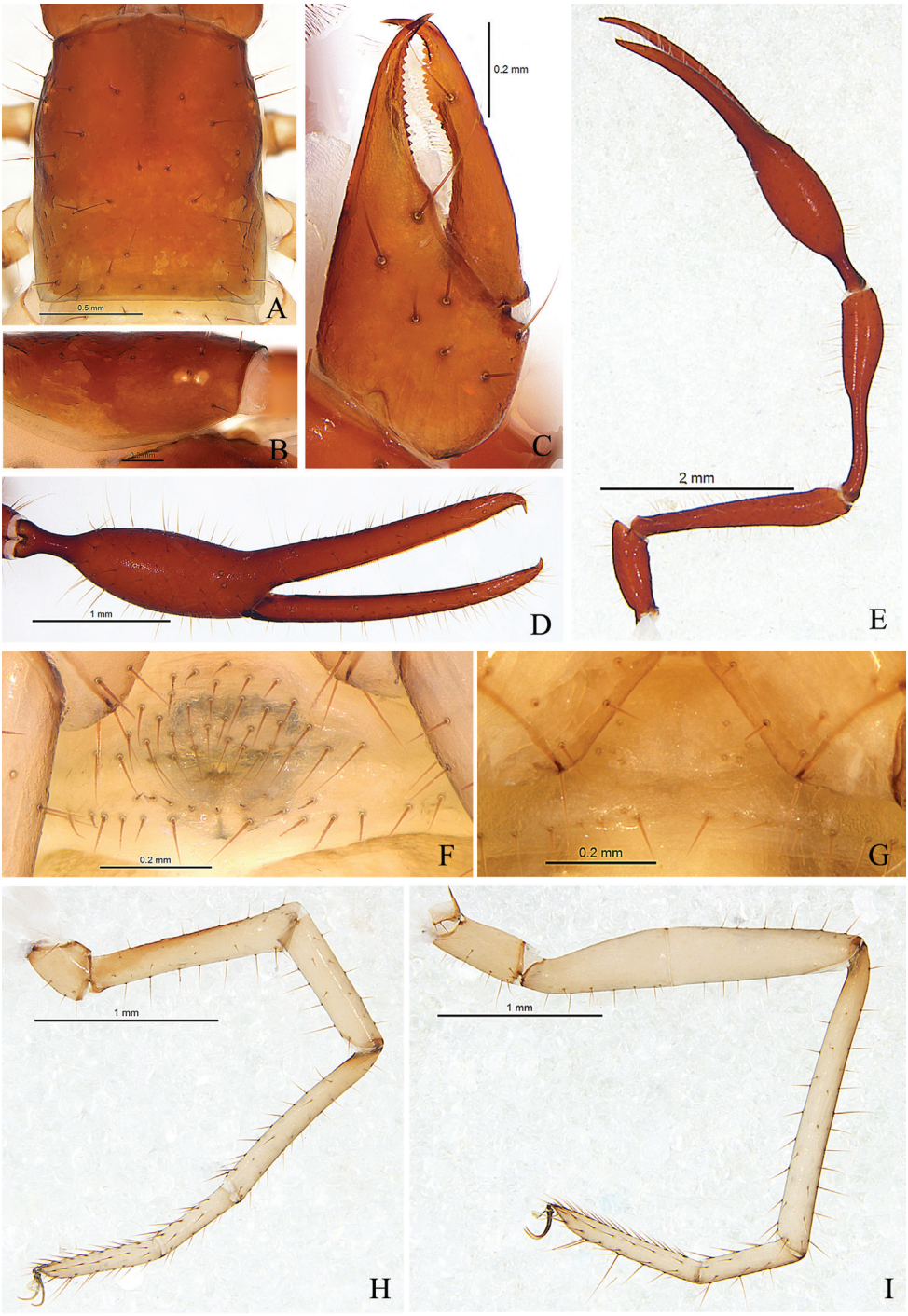

Figure 12. *Parobisium sanlouense* sp. nov., holotype male (**A**–**F**, **H**–**I**), female (**G**). **A** Carapace, dorsal view **B** Eye area, lateral view **C** Right chelicera, dorsal view **D** Right chela, lateral view **E** Right pedipalp, dorsal view **F** Male genitalia **G** Female genitalia **H** Right leg I, lateral view **I** Right leg IV, lateral view.

1.52 times longer than basitarsus. Leg IV (Figs 12I, 13M): femur + patella 5.22–5.97 times longer than deep, femur shorter than patella, tibia 8.95–9.10, basitarsus 4.06–4.19, telotarsus 6.93–6.86 times longer than deep, telotarsus 1.43–1.49 times longer basitarsus; basitarsus with one tactile setae (TS=0.12–0.13), telotarsus with one tactile setae (TS=0.43–0.52); subterminal tarsal seta (Fig. 13I) bifurcate, both branches dentate; arolium not divided, shorter than the slender and simple claws.

Female (paratypes) (Fig. 11B): Mostly same as holotype.

Chelicera. Hand with 7 setae, movable finger with 1 submedial seta; fixed finger with 13–16 teeth; movable finger with 14–15 teeth; serrula exterior with 37–41 lamellae; serrula interior with 23–27 lamellae. Galea (Fig. 13G) replaced by conspicuous semicircular transparent sclerotic knob; rallum of 8–10 blades, similar to that of holotype.

Pedipalps. Pedipalpal coxa with 8–9 setae. Trochanter 2.59–2.89, femur 6.03–6.60, patella 4.52–4.72, chela (with pedicel) 5.07–5.35, chela (without pedicel) 4.52–4.77 times longer than wide, movable finger 2.00–2.02 times longer than hand (without pedicel). Fixed chelal finger with 119–128 teeth, movable finger with 115–125 teeth.

Abdomen. Tergal chaetotaxy (I–XI): 6–9/8–11/10–11/9–11/9–10/10–11/11/10–11/10–11/9–11/7; sternal chaetotaxy (IV–XI): 8–9/12–13/12/12/12–14/12–14/12–13/3–4. Female genital area (Figs 12G, 13E): sternite II with 4–6 setae on each side; sternite III with a row of 12–15 setae on the posterior margin.

Measurements: (length/breadth or depth in mm; ratios for most characters in parentheses). Male (holotype and paratypes). Body length 4.00–4.79. Carapace 1.21–1.30 (1.32–1.42/1.09–1.09). Pedipalpal trochanter 2.86–2.92 (1.03–1.08/0.36–0.37), femur 6.50–6.59 (2.34–2.44/0.36–0.37), patella 5.07–5.11 (2.23–2.25/0.44), chela (with pedicel) 6.08–6.34 (3.59–3.68/0.58–0.59), chela (without pedicel) 5.44–5.62 (3.21–3.26/0.58–0.59), hand length (without pedicel) 1.34–1.38, movable finger length 2.08–2.11 (1.51–1.57 times longer than hand without pedicel). Leg I: trochanter 1.54–1.57 (0.43–0.44/0.28), femur 5.08–5.73 (1.22–1.26/0.22–1.24), patella 3.82–4.05 (0.84–0.85/0.21–0.22), tibia 8.21–8.57 (1.15–1.20/0.14), basitarsus 4.00–4.33 (0.52/0.12–0.13), telotarsus 6.08–6.58 (0.73–0.79/0.12). Leg IV: trochanter 2.41–2.55 (0.70–0.74/0.29), femur + patella 5.22–5.97 (1.93–2.09/0.35–0.37), tibia 8.95–9.10 (1.88–1.91/0.21), basitarsus 4.06–4.19 (0.65–0.67/0.16), telotarsus 6.93–6.86 (0.96–0.97/0.14).

Female (paratypes). Body length 4.94–6.00. Carapace 1.36–1.39 (1.51–1.54/1.11). Pedipalpal trochanter 2.59–2.89 (1.01–1.07/0.37–0.39), femur 6.03–6.60 (2.17–2.31/0.36–0.35), patella 4.52–4.72 (1.99–2.17/0.44–0.46), chela (with pedicel) 5.07–5.35 (3.40–3.48/0.65–0.67), chela (without pedicel) 4.52–4.77 (3.03–3.10/0.65–0.67), hand length (without pedicel) 1.31–1.34, movable finger length 1.87–2.00 (1.40–1.53 times longer than hand without pedicel). Leg I: trochanter 1.48–1.56 (0.40–0.42/0.27), femur 5.09–5.48 (1.12–1.26/0.22–0.23), patella 3.90–4.05 (0.78–0.81/0.20), tibia 7.20–8.14 (1.08–1.14/0.14–0.15), basitarsus 3.69–4.00 (0.48–0.52/0.13), telotarsus 5.21–6.08 (0.73–0.79/0.13–0.14). Leg IV: trochanter 2.10–2.64 (0.61–0.74/0.28–0.29), femur + patella 4.87–5.72 (1.90–2.06/0.36–0.39), tibia 8.48–9.05 (1.78–1.99/0.21–0.22), basitarsus 3.88–4.19 (0.66–0.67/0.16–0.17), telotarsus 6.50–7.07 (0.91–0.99/0.14).

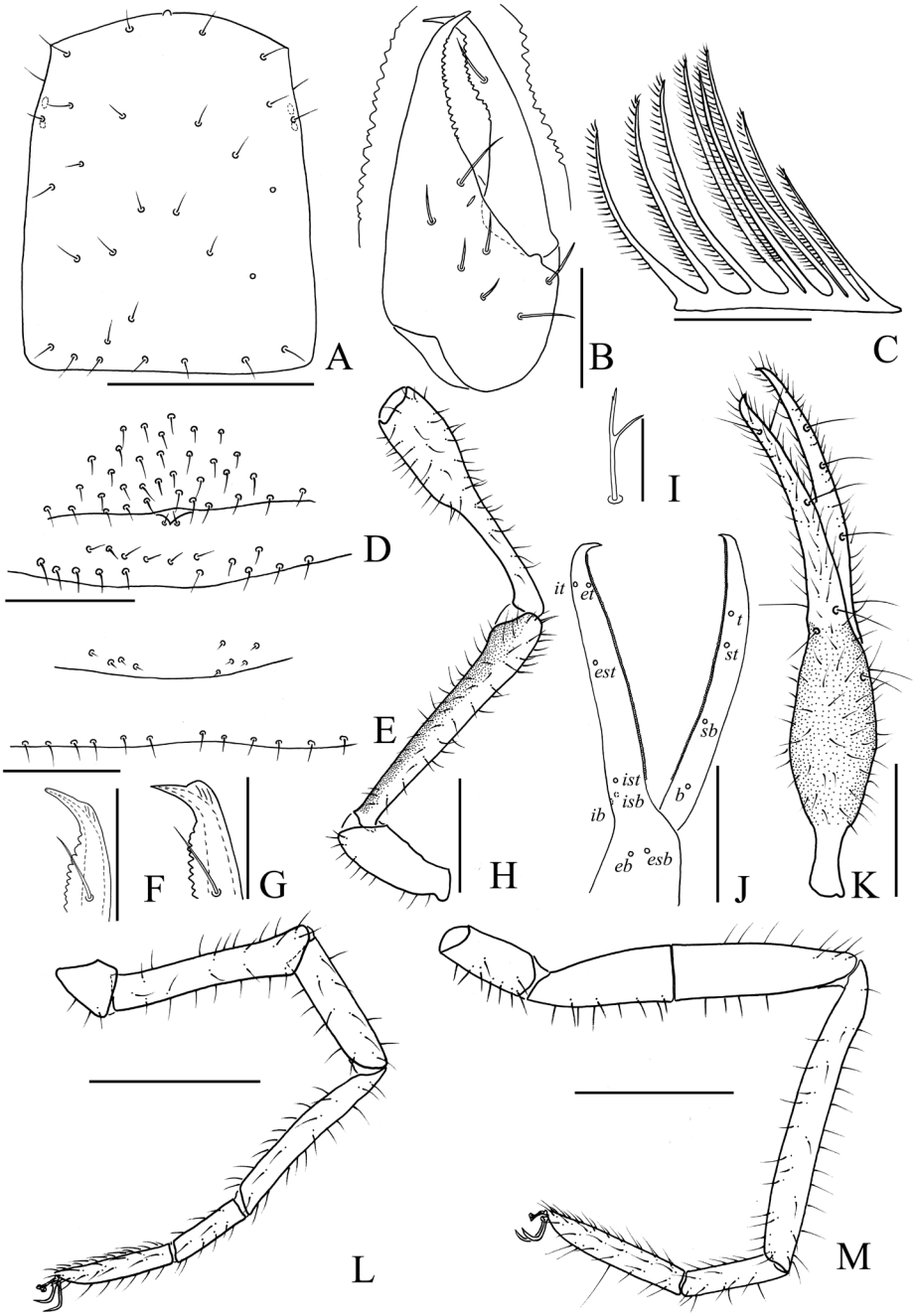

Figure 13. *Parobisium sanlouense* sp. nov., holotype male (**A**–**D**, **G**–**M**), female (**E**–**F**). **A** Carapace, dorsal view **B** Right chelicera, dorsal view **C** Rallum **D** Male genitalia **E** Female genitalia **F** Movable finger of chelicera (male), showing sclerotic knob **G** Movable finger of chelicera (female), showing sclerotic knob **H** Right pedipalp, dorsal view (trochanter, femur, and patella) **I** Subterminal tarsal seta **J** Right chelal fingers, lateral view **K** Right chela, dorsal view **L** Right leg I, lateral view **M** Right leg IV, lateral view. Scale bars: 0.5 mm (**A**–**B**), 0.1 mm (**C**, **I**), 0.25 mm (**D**–**G**), 1 mm (**H**, **J**–**M**).

***Parobisium tiani* sp. nov.**
http://zoobank.org/5E7363D4-BF81-401D-94A2-EA7D654FFBC1
Figs 14–17

Type material. Holotype male (Ps.-MHBU-GZ13070901): China, Guizhou Province, Liupanshui City, Pan County, Chengguan Town, Biyun Cave (Figs 1A, 21), [25°46'29.97"N, 104°38'15.81"E], 1500 m elevation, 9 July 2013, Mingyi Tian leg. Paratypes: 1 female (Ps.-MHBU-GZ13070902), same location as holotype, 09 July 2013, Mingyi Tian leg; 2 males (Ps.-MHBU-GZ19080501, GZ19080502), 2 females (Ps.-MHBU-GZ19080503, GZ19080504) same location as holotype, estimated cave deep zone, 05 August 2019, Zegang Feng, Chen Zhang leg.

Etymology. The name is a patronym to honor Chinese cave biologist, Mingyi Tian. He provided us with his pseudoscorpion specimens and assisted in developing this study.

Distribution. This species is known only from the type locality.

Diagnosis. This new troglomorphic species can be easily distinguished from other members of the genus *Parobisium* by following combination of characters: carapace with two faint eye spots (*P. wangae* has four developed eyes, *P. motianense, P. qiangzhuang* and *P. sanlouense* with four eye spots; *P. magangensis*, *P. xiaowutaicum* and *P. yuantongi* lacks eyes/eye spots); epistome triangular, with rounded top (small, rounded in *P. motianense*, *P. qiangzhuang* and *P. sanlouense*; triangular, with rounded top in *P. tiani* and *P. yuantongi*; rounded in *P. magangensis* and *P. xiaowutaicum*); pedipalpal femur 5.63–5.75 times longer than wide (8.91–8.97 times in *P. magangensis*; 4.66–4.90 times in *P. motianense*; 3.89–4.11 times in *P. qiangzhuang*; 6.50–6.59 times in *P. sanlouense*; 3.60–3.65 times in *P. wangae*; 4.65 times in *P. xiaowutaicum*; 6.75 times in *P. yuantongi*); patella 4.52–4.58 times longer than wide (7.64–7.84 times in *P. magangensis*; 3.09–3.39 times in *P. motianense*; 2.54–2.60 times in *P. qiangzhuang*; 5.07–5.11 times in *P. sanlouense*; 1.89–2.16 times in *P. wangae*; 3.14 times in *P. xiaowutaicum*; 5.70 times in *P. yuantongi*); pedipalpal hand with granulation (smooth in *P. magangensis*, *P. wangae* and *P. xiaowutaicum*; with granulation present on chelal hand in *P. tiani*; with granulation present on inside lateral of femur and chelal hand in *P. qiangzhuang* and *P. sanlouense*; with granulation present on femur, inside lateral of patella and chelal hand in *P. yuantongi*); chela (with pedicel) 4.97–5.03 times longer than wide (8.67–8.69 times in *P. magangensis*; 3.72–4.06 times in *P. motianense*; 3.12–3.25 times in *P. qiangzhuang*; 6.08–6.34 times in *P. sanlouense*; 3.13–3.52 times in *P. wangae*; 3.14 times in *P. xiaowutaicum*; 5.70 times in *P. yuantongi*); both chelal finger has 104–112 teeth (146–162 in *P. magangensis*; 71–75 in *P. qiangzhuang*; 57–74 in *P. wangae*; 73–75 in *P. xiaowutaicum*).

Description. Male (Fig. 15A). Carapace, chelicerae, and pedipalps reddish brown or yellowish brown; abdomen and legs yellowish or yellowish brown.

Carapace (Figs 16A, 17A): Smooth, 1.22–1.27 times longer than broad, with a total of 24 setae, including 4 on anterior margin, 6 on posterior margin, and 1 on each side of anterior lateral margin; with 2 faint eye spots on a flat surface; epistome triangular, with rounded top.

Figure 14. *Parobisium tiani* sp. nov. Male habitus.

Chelicera (Figs 16C, 17B): Hand with 7 setae, movable finger with 1 submedial seta; fixed finger with 13–16 teeth; movable finger with 13–16 teeth; serrula exterior with 39–42 lamellae; serrula interior with 20–24 lamellae. Galea (Fig. 17D) replaced by a small rounded transparent sclerotic knob. Rallum (Fig. 17C) with 8 pinnate blade, distal-most blade with expanded base, and together with the second blade separated from the others, proximal one short.

Pedipalps (Figs 16E–F, 17H–I, K): Apex of coxa rounded, with 5 setae on each side, pedipalpal coxa with 7–8 setae. Pedipalp smooth and slender except for hand, which is finely granular. Trochanter 2.67–2.70 times longer than wide, femur 5.63–5.73, patella 4.52–4.58 times longer than wide, pedicel about half the entire length of patella, chela (with pedicel) 4.97–5.03, chela (without pedicel) 4.39–4.40 times longer than wide, movable finger 1.44–1.45 times longer than hand (without pedicel). Fixed chelal finger with 8 trichobothria, movable finger with 4, *eb* and *esb* on lateral margin of hand; *ib*, *ist* and *isb* closely grouped at the base of the fixed finger; *est* slightly distal of finger middle; *it* closer to fingertip than *et*; on movable finger, *st* nearer to *t* than to *sb*, the latter slightly nearer *st* than to *b* (Figs 16F, 17H–I). Venom apparatus present only in fixed chelal finger, venom duct short, not extending past half of the distance to *et*. Fixed chelal finger with 104–109 teeth, movable finger with 105–112 teeth.

Abdomen: Pleural membrane granulated. Tergal chaetotaxy (I–XI): 8–9/ 8–9/ 9/ 10/ 9/ 9–11/ 9–10/ 10–11/ 10–12/ 10–11/ 6–7; sternal chaetotaxy (IV–XI): 7–8/ 12–13/ 14/ 12–13/ 11–13/ 11–12/ 11–12/ 3–4; stigmata with 5–6 setae; anal cone with 2 dorsal and 2 ventral setae. Male genital area (Figs 16G, 17F): sternite II with

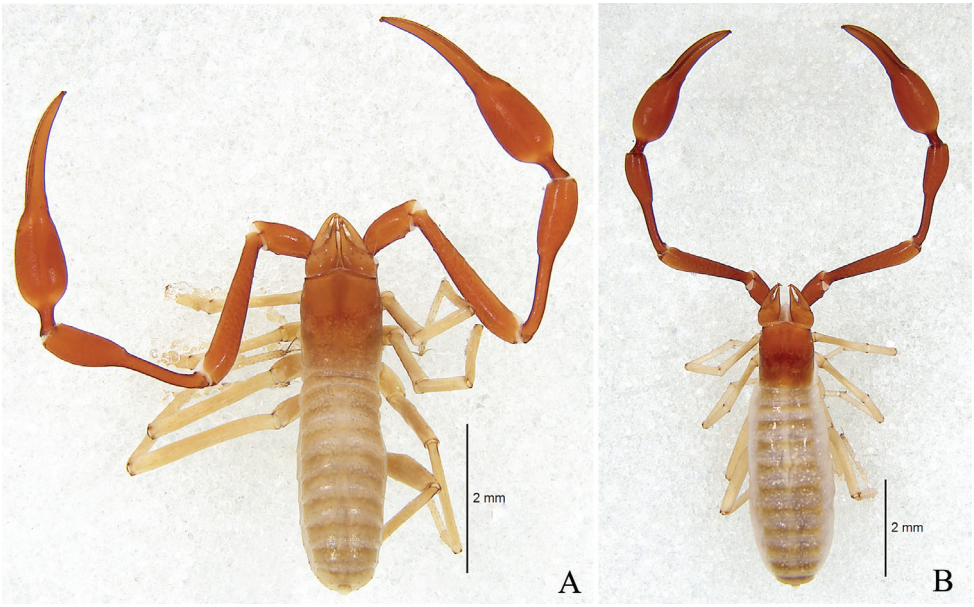

Figure 15. *Parobisium tiani* sp. nov. **A** Holotype male, dorsal view **B** Paratype female, dorsal view.

34–43 scattered setae; sternite III with anteromedian groove flanked by one small seta on each side, with 15 posterior setae.

Legs: Coxa chaetotaxy (I–IV): 6–7/ 4–5/ 4–5/ 7. Leg I (Figs 16I, 17L): femur 6.27–6.50, patella 3.54–4.23, tibia 8.87–9.08, basitarsus 3.73–3.93, telotarsus 5.07–5.85 times longer than deep, femur 1.54–1.62 times longer than patella, telotarsus 1.36–1.38 times longer than basitarsus. Leg IV (Figs 16J, 17M): femur + patella 5.30–5.46 times longer than deep, femur shorter than patella, tibia 9.04–9.75, basitarsus 4.06–4.41, telotarsus 5.61–6.20 times longer than deep, telotarsus 1.35 times longer than basitarsus; basitarsus with a tactile setae in basally (TS=0.12–0.15), telotarsus with a tactile setae in middle (TS=0.46–0.47); subterminal tarsal seta (Fig. 17J) bifurcate, both branches dentate; arolium not divided, shorter than the slender and simple claws.

Female (paratypes) (Fig. 15B): Mostly same as holotype.

Chelicera. Hand with 7 setae, movable finger with 1 submedial seta; fixed finger with 13–16 teeth; movable finger with 12–19 teeth; serrula exterior with 39–41 lamellae; serrula interior with 22–23 lamellae. Galea (Fig. 17E) replaced by a semicircular transparent sclerotic knob; rallum of 8–9 blades, similar to holotype.

Pedipalps. Trochanter 2.44–2.61, femur 5.59–5.61, patella 4.38–4.57 times longer than wide; chela (with pedicel) 4.25–4.46 times longer than wide, chela (without pedicel) 3.79–4.00 times longer than wide, movable finger 1.26–1.28 times longer than hand (without pedicel). Fixed chelal finger with 96–106 teeth, movable finger with 97–105 teeth.

Abdomen. Tergal chaetotaxy (I–XI): 6–7/ 7–9/ 8–9/ 8–10/ 9–11/ 10–12/ 9–12/ 9–12/ 11–12/ 11/ 6–7; sternal chaetotaxy (IV–XI): 8–9/ 13–15/ 13–16/ 13–15/ 13–

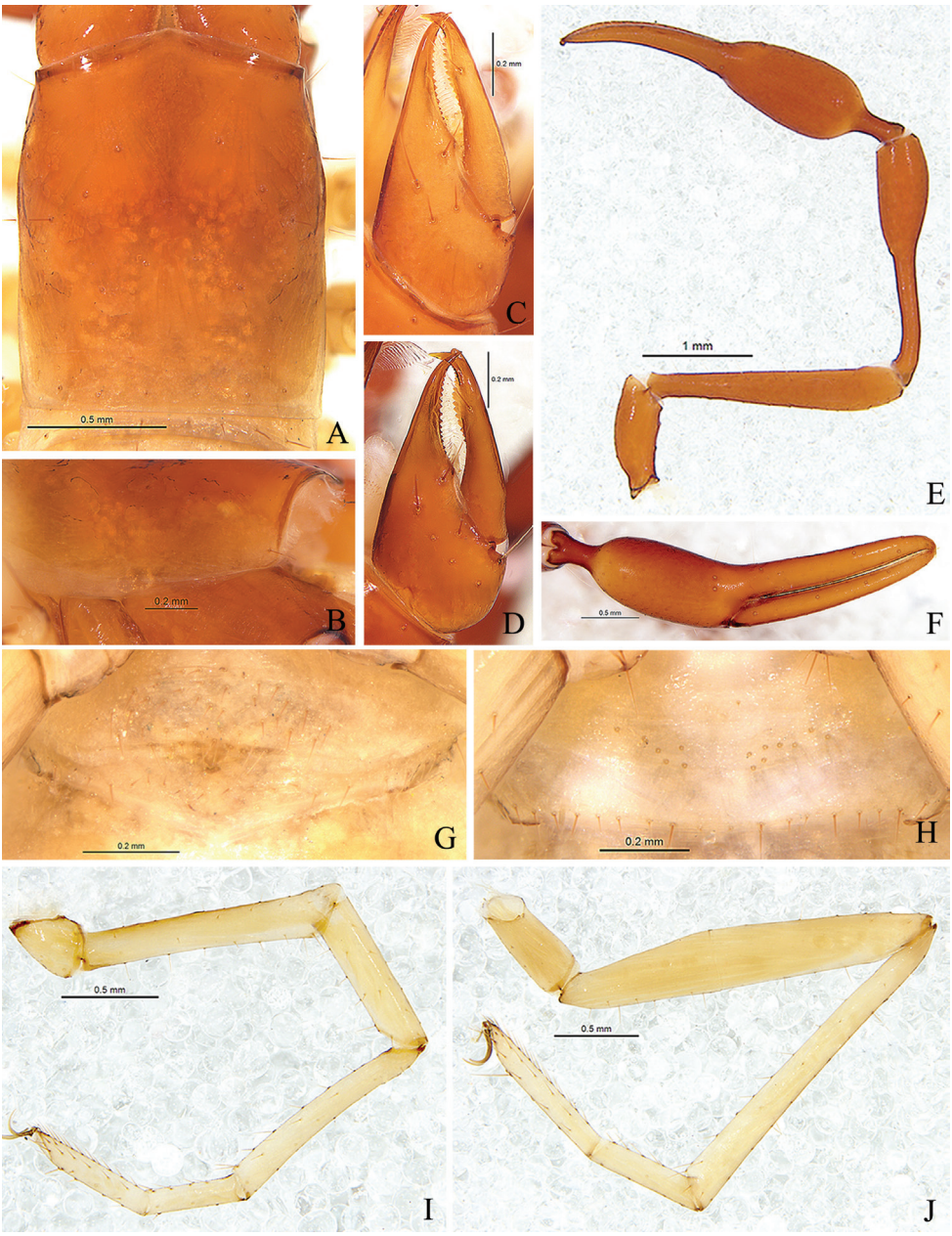

Figure 16. *Parobisium tiani* sp. nov., holotype male (**A**–**C**, **E**–**G**, **I**–**J**), female (**D**, **H**). **A** Carapace, dorsal view **B** Eye area, lateral view **C** Right chelicera of male, dorsal view **D** Right chelicera of female, dorsal view **E** Right pedipalp, dorsal view **F** Right chela, lateral view **G** Male genitalia **H** Female genitalia **I** Right leg I, lateral view **J** Right leg IV, lateral view.

15/ 12–13/ 12–14/ 3. Female genital area (Figs 16H, 17G): sternite II with 3–8 setae on each side; sternite III with a row of 13–16 setae on the posterior margin.

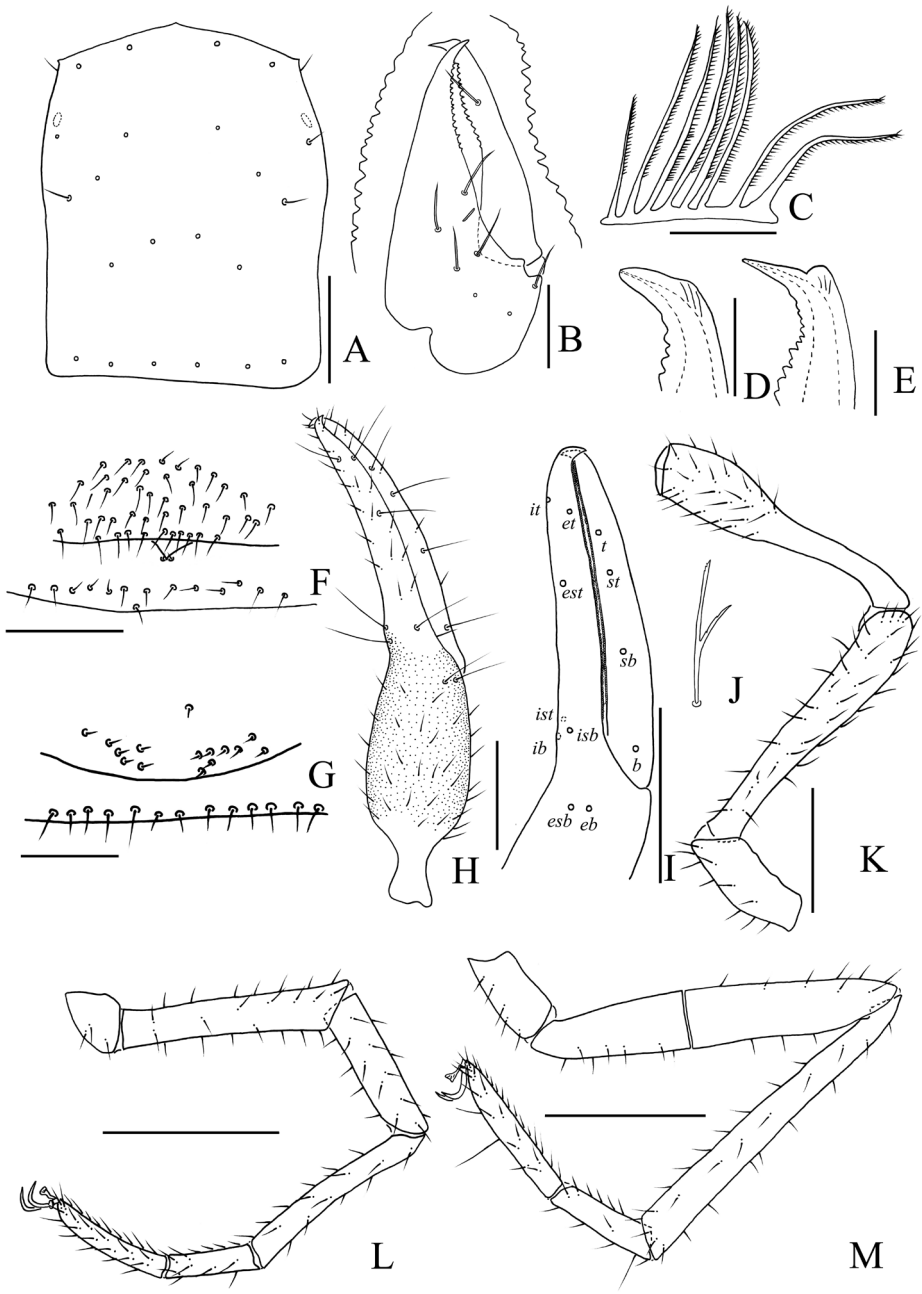

Figure 17. *Parobisium tiani* sp. nov., holotype male (**A–D**, **F**, **H–M**), female (**E**, **G**). **A** Carapace, dorsal view **B** Right chelicera, dorsal view **C** Rallum **D** Movable finger of chelicera (male), showing sclerotic knob **E** Movable finger of chelicera (female), showing sclerotic knob **F** Male genitalia **G** Female genitalia **H** Right chela, dorsal view **I** Right chelal fingers, lateral view **J** Subterminal tarsal seta **K** Right pedipalp, dorsal view (trochanter, femur, and patella) **L** Right leg I, lateral view **M** Right leg IV, lateral view. Scale bars: 0.1 mm (**C**–**E**, **J**), 0.25 mm (**B**, **F**–**G**), 0.5 mm (**A**), 1 mm (**H**–**I**, **K**–**M**).

Measurements: (length/breadth or depth in mm; ratios for most characters in parentheses). Male (holotype and paratypes). Body length 3.87–5.09. Carapace 1.22–1.27 (1.32–1.43/1.08–1.13). Pedipalpal trochanter 2.67–2.70 (1.04–1.16/0.39–0.43), femur 5.63–5.73 (2.29–2.42/0.40–0.43), patella 4.52–4.58 (2.17–2.38/0.48–0.52), chela (with pedicel) 4.97–5.03 (3.28–3.52/0.66–0.70), chela (without pedicel) 4.39–4.40 (2.90–3.08/0.66–0.70), hand length (without pedicel) 1.32–1.36, movable finger length 1.91–1.96 (1.44–1.45 times longer than hand without pedicel). Leg I: trochanter 1.35–1.50 (0.42/0.28–0.31), femur 6.27–6.50 (1.38–1.43/0.22), patella 3.54–4.23 (0.85–0.93/0.22–0.24), tibia 8.87–9.08 (1.18–1.33/0.13–0.15), basitarsus 3.73–3.93 (0.55–0.56/0.14–0.15), telotarsus 5.07–5.85 (0.76/0.13–0.15). Leg IV: trochanter 2.43–2.79 (0.68–0.78/0.28), femur + patella 5.30–5.46 (2.13–2.28/0.39–0.43), tibia 9.04–9.75 (2.17–2.34/0.24), basitarsus 4.06–4.41 (0.69–0.75/0.17), telotarsus 5.61–6.20 (0.93–1.01/0.15–0.18).

Female (paratypes). Body length 4.63–5.48. Carapace 1.19–1.27 (1.30–1.60/1.09–1.26). Pedipalpal trochanter 2.44–2.61 (0.95–1.15/0.39–0.44), femur 5.59–5.61 (2.18–2.47/0.39–0.44), patella 4.38–4.57 (2.06–2.47/0.47–0.54), chela (with pedicel) 4.25–4.46 (3.03–3.61/0.68–0.85), chela (without pedicel) 3.79–4.00 (2.72–3.22/0.68–0.85), hand length (without pedicel) 1.29–1.55, movable finger length 1.65–1.95 (1.26–1.28 times longer than hand without pedicel). Leg I: trochanter 1.47–1.60 (0.40–0.44/0.25–0.30), femur 5.39–5.92 (1.24–1.48/0.23–0.25), patella 3.75–4.18 (0.75–0.92/0.20–0.22), tibia 7.00–7.33 (1.05–1.32/0.15–0.18), basitarsus 3.14–4.07 (0.44–0.61/0.14–0.15), telotarsus 5.00–5.43 (0.65–0.76/0.13–0.14). Leg IV: trochanter 2.48–2.61 (0.67–0.81/0.27–0.31), femur + patella 5.91–5.97 (2.01–2.27/0.34–0.38), tibia 9.38–9.67 (1.97–2.32/0.21–0.24), basitarsus 3.82–4.53 (0.65–0.77/0.17), telotarsus 6.00–6.13 (0.90–0.98/0.15–0.16).

Discussion

Our work has increased the number of Chinese cave-dwelling pseudoscorpions from 25 to 29 species. In addition, we found that female individuals may have a distinctly rounded sclerotic knob, while the sclerotic knob in males was not often obvious. Uncertainty of the characteristics of the sclerotic knob makes versus the damaged of galeae it difficult to identify and describe species – especially when only a single-sex specimen is available. We recommend that future researchers: (1) collect multiple specimens to help ensure both adult males and females are collected (enabling further examination and study of the sclerotic knob across additional specimens and species); (2) carefully collect pseudoscorpions to avoid damaging the galeae; (3) cautiously examine the galeae particularly when specimens are few; and, (4) use scanning electron microscopy (e.g., Cokendolpher and Krejca 2010) to more accurately examine the structure of the galeae. The latter will enable researchers to determine whether galea are reduced or altered during collection or transportation.

As with most Chinese hypogean pseudoscorpions (Table 1; Schawaller 1995; Mahnert 2003, 2009; Mahnert and Li 2016; Gao et al. 2017; Li et al. 2017; Gao et al.

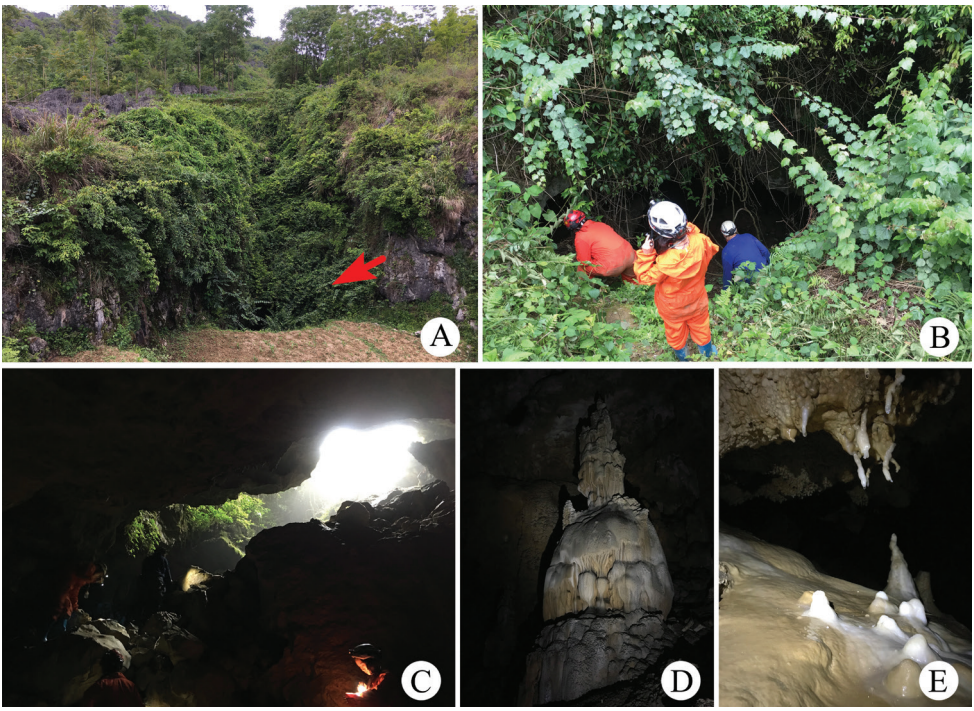

Figure 18. Motian Cave, type locality of *Parobisium motianense* sp. nov. **A** Surrounding vegetation and agricultural areas with cave entrance (Red arrow) **B** Entrance **C** Inside the cave entrance **D** Stalactites **E** Cave landscape.

2018; Feng et al. 2019; Li et al. 2019), these four new species are currently considered single cave endemics. However, this may be due to limited investigations in the region, rather than actual short-range distributions of these species. There is a high density of caves in Guizhou – in particular, numerous caves occur within a 5 km radius of the caves containing these species. Specifically, there are at least three caves with a 5 km radius of Zhaorou Cave, no fewer than seven caves with a 5 km radius of the Sanlou Cave, and at least 10 caves with a 5 km radius in Biyun Cave. None of these caves have been inventoried for cave-dwelling arthropods. As a result, it is possible our newly described species are actually restricted to a geological formation rather than a single cave (Schawaller 1995; Mahnert 2009; Mahnert and Li 2016; Table 1). Additional investigations will be required to make this distinction.

While it is becoming increasingly well-established that caves in China are rich in cave biological resources and support subterranean-adapted species with highly restricted distributional ranges, the county presently lacks policies or a governmental agency to protect and manage subterranean natural resources. This presents challenges for conservation and management of sensitive subterranean animal populations. Unfortunately, human activities (i.e., urbanization, mining, and other related activities) in karst areas, and the development of tourist caves, continue without prior evaluations of the potentially sensitive natural resources and/or the biodiversity they may support

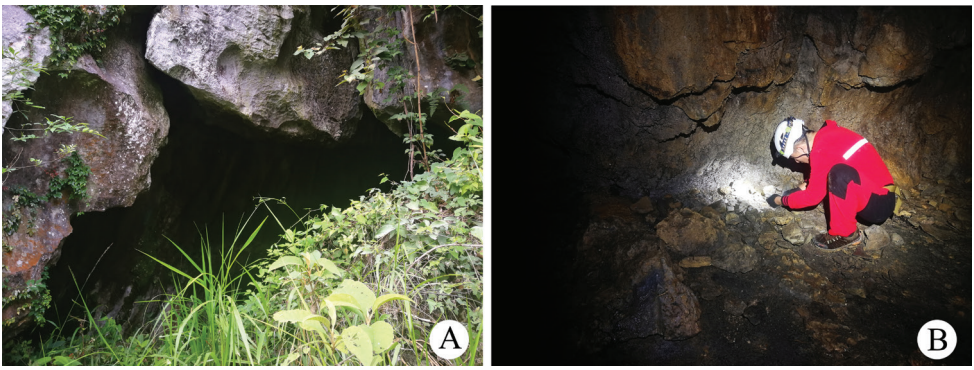

Figure 19. Zharou Cave, type locality of *Parobisium qiangzhuang* sp. nov. **A** entrance **B** Area where *P. qiangzhuang* specimens were collected.

(Whitten 2009). Therefore, we recommend the distributions of the new species described here be more thoroughly established through sampling of the abovementioned caves surrounding the type localities. Importantly, once we determine whether these species are single cave or regional endemics, this information may be used to guide management policies to protect these animals and their habitats.

Local human activities (Figs 20A, D, 21D) are more likely to have significant impacts on these cave-dwelling species, which could result in their imperilment or potentially their extinction. In fact, the four new Guizhou pseudoscorpions and their habitats are directly threatened by human activities. All four caves were close to human settlements and/or agricultural areas (within 0 m to 100 m) and were affected to varying degrees by other human activities. Motian Cave is surrounded by agricultural activities. For Zharou Cave, agricultural activities are less than 100 m away. In both cases, pesticide and fertilizer residues may contaminate the caves via runoff (Castaño-Sánchez et al. 2019). Although the entrance of Zharou Cave is somewhat obscured by vegetation, local residents are aware of this cave, and we observed recent evidence of human activities. The entrance of the Sanlou Cave is about 50 m from sand mining operations, and the deepest part of the cave has been modified and converted to a reservoir. Additionally, the sand mining facility and the water extraction activities may ultimately affect the survival of *P. sanlouense* sp. nov.

Biyun Cave, located in Biyun county park, is a tourist cave. Evidence of human activity was observed throughout the cave, which included refuse, remnants of bonfires, and graffiti on the cave walls. Subsequently, cave habitats have been damaged to varying degrees. During our work, we observed at least 10 tourists visiting the cave. Fortunately, because of the muddy and steep path at the back of the cave, we suspect fewer visitors will be willing to access the area where we found *P. tiani* sp. nov. As a result, this habitat may be somewhat protected.

Extinction is often characterized by time lags, and at-risk populations may persist for long periods of time near extinction thresholds prior to becoming extinct (e.g., Brooks et al. 1999, Hanski and Ovaskainen 2002, Vellend et al. 2006). These "ex-

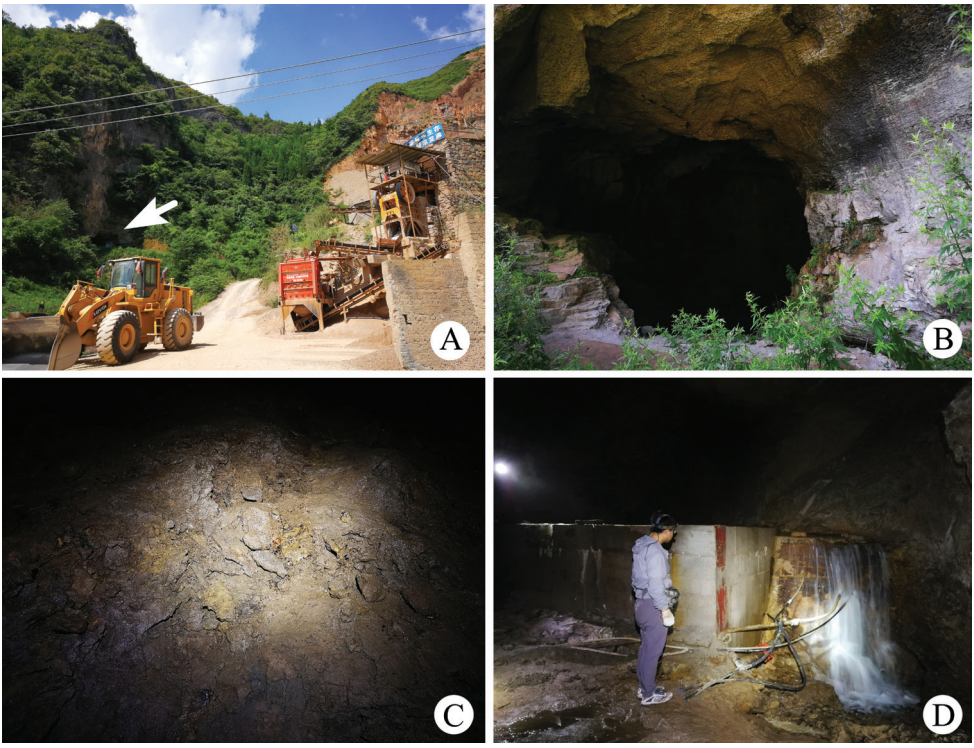

Figure 20. Sanlou Cave, type locality of *Parobisium sanlouense* sp. nov. **A** Surrounding surface vegetation with cave entrance (white arrow) and sand mining operations adjacent to the cave **B** Entrance **C** Area where *P. sanlouense* specimens were collected **D** Terminus of Sanlou Cave with the potable water reservoir; specimens were collected near the reservoir.

tinction debts" (see Tilman et al. 1994) may occur when populations become isolated following significant environmental perturbations or intensive human activities. Both *P. sanlouense* sp. nov. and *P. tiani* sp. nov. occur in areas of intensive human activities. This further emphasizes the need for additional surveys to determine whether these species are single cave or regional endemics. This distinction will be of critical importance in determining the sensitivity of these animals to current human activities within and at proximity to the caves where they occur. Moreover, understanding their distributions will be required to develop effective monitoring protocols – if additional evidence supports that either (or both) species are single cave endemics.

There are other measures that should be examined to protect sensitive cave-dwelling species and their habitats. An outreach campaign to help educate villagers, school children, and tourists concerning the vulnerability of cave biological resources should be considered (refer to Mammola et al. 2019). At Biyun Cave, it may be worth posting educational signs (within the village and perhaps near the entrance) to explain the sensitivity of cave natural resources and that endemic species occur within, as well as guidelines for reducing human impacts to sensitive cave resources.

Figure 21. Biyun Cave, type locality of *Parobisium tiani* sp. nov. **A** Surrounding surface habitat with two entrances, entrance 1 (white arrow) and entrance 2 (red arrow) **B** Entrance 1 (white arrow) **C** Entrance 2 (red arrow) **D** Passage where specimens were collected (blue arrow).

As research on cave biological resources in southern China continues, numerous additional new species with restricted ranges will be described. Understanding their distributions and the functional roles they play in these often highly sensitive ecological communities will be of paramount importance for developing management plans to protect both sensitive species and their habitat. Through these and other efforts, we hope our findings and data collected in the future will be employed to help shape effective cave resource management in China.

Acknowledgments

We are grateful to Mingyi Tian for contributing specimens and providing us with information and images (Figs 2, 18), on the caves he sampled. This work was supported by the National Natural Science Foundation of China (No. 31872198), and the Ministry of Science and Technology of the People's Republic of China (MOST Grant No. 2015FY210300).

References

Barr Jr TC (1967) Observations on the ecology of caves. American Naturalist 101: 475–491. https://doi.org/10.1086/282512

Beier M (1932) Pseudoscorpionidea I. Subord. Chthoniinea et Neobisiinea. Tierreich 57: 1–258. https://doi.org/10.1515/9783111435107

Borges PAV, Cardoso P, Amorim IR, Pereira F, Constância JP, Nunes JC, Barcelos P, Costa P, Gabriel R, Dapkevicius ML (2012) Volcanic caves: priorities for conserving the Azorean endemic troglobiont species. International Journal of Speleology 41: 101–112. https://doi.org/10.5038/1827-806X.41.1.11

Brooks TM, Pimm SL, Oyugi JO (1999) Time lag between deforestation and bird extinction in tropical forest fragments. Conservation Biology 13: 1140–1150. https://doi.org/10.1046/j.1523-1739.1999.98341.x

Castaño-Sánchez A, Hose GC, Reboleira ASPS (2019) Ecotoxicological effects of anthropogenic stressors in subterranean organisms: A review. Chemosphere 125422. https://doi.org/10.1016/j.chemosphere.2019.125422

Chamberlin JC (1930) A synoptic classification of the false scorpions or chela-spinners, with a report on a cosmopolitan collection of the same. Part II. The Diplosphyronida (Arachnida-Chelonethida). Annals and Magazine of Natural History (10) 5: 1–48. https://doi.org/10.1080/00222933008673104

Chamberlin JC (1931) The arachnid order Chelonethida. Stanford University Publications. Biological Sciences 7: 1–284.

Chamberlin JC (1962) New and little-known false scorpions, principally from caves, belonging to the families Chthoniidae and Neobisiidae (Arachnida, Chelonethida). Bulletin of the American Museum of Natural History 123: 303–352.

Chamberlin JC, Malcolm DR (1960) The occurrence of false scorpions in caves with special reference to cavernicolous adaptation and to cave species in the North American fauna (Arachnida-Chelonethida). American Midland Naturalist 64: 105–115. https://doi.org/10.2307/2422895

Chevaldonné P, Lejeune C (2003) Regional warming-induced species shift in north-west Mediterranean marine caves. Ecology Letters 6: 371–379. https://doi.org/10.1046/j.1461-0248.2003.00439.x

Christman MC, Culver DC, Madden MK, White D (2005) Patterns of endemism of the eastern North American cave fauna. Journal of Biogeography 32: 1442–1452. https://doi.org/10.1111/j.1365-2699.2005.01263.x

Clements R, Sodhi NS, Schilthuizen M, Ng PK (2006) Limestone karsts of Southeast Asia: imperiled arks of biodiversity. Bioscience 56: 733–742. https://doi.org/10.1641/0006-3568(2006)56%5B733:LKOSAI%5D2.0.CO;2

Cokendolpher JC, Krejca JK (2010) A new cavernicolous *Paribisium* Chamberlin 1930 (Pseudoscorpiones: Neobisiidae) from Yosemite National Park, U.S.A., Museum of Texas Tech University 297: 1–25. https://doi.org/10.5962/bhl.title.156953

Culver DC, Master LL, Christman MC, Hobbs HH III (2000) Obligate cave fauna of the 48 contiguous United States. Conservation Biology 14: 386–401. https://doi.org/10.1046/j.1523-1739.2000.99026.x

Ćurčić BPM (1983) A revision of some Asian species of *Microcreagris* Balzan, 1892 (Neobisiidae, Pseudoscorpiones). Bulletin of the British arachnological Society 6 (1): 23–36.

Deuve T, Tian MY (2018) Nouveaux Trechini cavernicoles du Guizhou ord-occidental des genres Zhijinaphaenops et Guizhaphaenops (Coleoptera, Trechidae). Bulletin de la Société entomologique de France 123 (3): 333–339. https://doi.org/10.32475/bsef_2039

Feng ZG, Wynne JJ, Zhang F (2019) Two new subterranean-adapted pseudoscorpions (Pseudoscorpiones: Neobisiidae: *Parobisium*) from Beijing, China. Zootaxa 4661 (1): 145–160. https://doi.org/10.11646/zootaxa.4661.1.7

Ferreira RL, Horta LCS (2001) Natural and human impacts on invertebrate communities in Brazilian caves. Revista Brasileira de Biologia 61: 7–17. https://doi.org/10.1590/S0034-71082001000100003

Fišer C, Zagmajster M, Zakšek V (2013) Coevolution of life history traits and morphology in female subterranean amphipods. Oikos 122: 770–778. https://doi.org/10.1111/j.1600-0706.2012.20644.x

Gao ZZ, Chen HM, Zhang F (2017) Description of two new cave-dwelling *Bisetocreagris* species (Pseudoscorpiones: Neobisiidae) from China. Turkish Journal of Zoology 41: 615–623. https://doi.org/10.3906/zoo-1602-39

Gao ZZ, Wynne JJ, Zhang F (2018) Two new species of cave-adapted pseudoscorpions (Pseudoscorpiones: Neobisiidae, Chthoniidae) from Guangxi, China. Journal of Arachnology 46: 345–354. https://doi.org/10.1636/JoA-S-17-063.1

Guo XB, Zhang F (2016) Two new species of the genus *Parobisium* Chamberlin, 1930 from China (Pseudoscorpiones: Neobisiidae). Entomologica Fennica 27: 140–148.

Hanski I, Ovaskainen O (2002) Extinction debt at extinction threshold. Conservation Biology 16: 666–673. https://doi.org/10.1046/j.1523-1739.2002.00342.x

Harley GL, Polk JS, North LA, Reeder PP (2011) Application of a cave inventory system to stimulate development of management strategies: The case of west-central Florida, USA. Journal of Environmental Management 92: 2547–2557. https://doi.org/10.1016/j.jenvman.2011.05.020

Harvey MS (1991) Catalogue of the Pseudoscorpionida. Manchester University Press: Manchester, Pp. 850.

Harvey MS (1992) The phylogeny and classification of the Pseudoscorpionida (Chelicerata: Arachnida). Invertebrate Taxonomy 6: 1373–1435. https://doi.org/10.1071/IT9921373

He W, Li P (2016) Resources features of Guizhou Karst cave and development and utilization. Journal of Guizhou Normal University (Natural Sciences) 2016, 34 (03): 1–6 (in Chinese with English abstract). https://doi.org/10.16614/j.cnki.issn1004-5570.2016.03.001

Hoff CC (1961) Pseudoscorpions from Colorado. Bulletin of the American Museum of Natural History 122: 409–464.

Hong Y (1996) Two new species of the genus *Parobisium* (Pseudoscorpionida: Neobisiidae) from Korea. Korean Journal of Systematic Zoology 12: 189–197.

Huang SB, Cen YJ, Tian MY (2017) A new genus and a new subgenus of cavernicolous beetles from Furong Jiang valley, southwestern China (Coleoptera: Carabidae: Trechinae). Annales de la Société entomologique de France (N.S.) 53 (4): 286–295. https://doi.org/10.1080/00379271.2017.1344566

Howarth FG (1980) The zoogeography of specialized cave animals: A bioclimatic model. Evolution 34: 394–406. https://doi.org/10.1111/j.1558-5646.1980.tb04827.x

Howarth FG (1983) Ecology of cave arthropods. Annual Review of Entomology 28: 365–389. https://doi.org/10.1146/annurev.en.28.010183.002053

Howarth FG, James SA, McDowell W, Preston DJ, Imada CT (2007) Identification of roots in lava tube caves using molecular techniques: Implications for conservation of cave arthropod faunas. Journal of Insect Conservation 11: 251–261. https://doi.org/10.1007/s10841-006-9040-y

Judson MLI (2007) A new and endangered species of the pseudoscorpion genus *Lagynochthonius* from a cave in Vietnam, with notes on chelal morphology and the composition of the Tyrannochthoniini (Arachnida, Chelonethi, Chthoniidae). Zootaxa 1627: 53–68. https://doi.org/10.11646/zootaxa.1627.1.4

Kováč ĽU, Mock AN, Ľuptáčik PE, Košel VL, Fenďa PE, Svatoň J, Mašán P (2005) Terrestrial arthropods of the Domica Cave system and the Ardovská Cave (Slovak Karst)–principal microhabitats and diversity. 7th Central European Workshop on Soil Zoology, April 14-16, 2003, In *Contributions to Soil Zoology in Central Europe I*, *České Budějovice*, 61–70.

Li B, Zhao Z, Zhang C, Li S (2019a) *Troglocoelotes* gen. n., a new genus of Coelotinae spiders (Araneae, Agelenidae) from caves in South China. Zootaxa 4554 (1): 219–238. https://doi.org/10.11646/zootaxa.4554.1.7

Li SQ, Wang XX (2017) New cave-dwelling spiders of the family Dictynidae (Arachnida: Araneae) from Guangxi and Guizhou, China. Zoological Systematics 42 (2): 125–228

Li YC, Shi AM, Liu H (2017) A new cave-dwelling species of *Bisetocreagris* (Arachnida, Pseudoscorpiones: Neobisiidae) from Yunnan Province, China. Entomol. Fennica 28: 212–218. https://doi.org/10.33338/ef.84688

Li YC, Liu H, Shi AM (2019b) A new cave-dwelling species of *Lagynochthonius* (Arachnida: Pseudoscorpiones: Chthoniidae) from Yunnan Province, China. Zootaxa 4571 (1): 28–34. https://doi.org/10.11646/zootaxa.4571.1.2

Mahnert V (2003) Four new species of pseudoscorpions (Arachnida, Pseudoscorpiones: Neobisiidae, Chernetidae) from caves in Yunnan Province, China. Revue Suisse de Zoologie 110: 739–748. https://doi.org/10.5962/bhl.part.80209

Mahnert V (2009) New species of pseudoscorpions (Arachnida, Pseudoscorpiones, Chthoniidae, Chernetidae) from caves in China. Revue Suisse de Zoologie 116: 185–201. https://doi.org/10.5962/bhl.part.79492

Mahnert V, Li YC (2016) Cave-inhabiting Neobisiidae (Arachnida: Pseudoscorpiones) from China, with description of four new species of *Bisetocreagris* Ćurčić. Revue Suisse de Zoologie 123: 259–268.

Mammola S, Cardoso P, Culver DC, Deharveng L, Ferreira RL, Fišer C, Galassi DPM, Griebler C, Halse S, Humphreys WF, Isaia M, Malard F, Martinez A, Moldovan OT, Niemiller ML, Pavlek M, Reboleira ASPS, Souza-Silva M, Teeling EC, Wynne JJ, Zagmajster M (2019) Scientists' warning on the conservation of subterranean ecosystems. BioScience 69 (8): 641–650. https://doi:10.1093/biosci/biz064.

Mammola S, Goodacre SL, Isaia M (2018) Climate change may drive cave spiders to extinction. Ecography 41: 233–243.https://doi.org/10.1111/ecog.02902

Morikawa K (1960) Systematic studies of Japanese pseudoscorpions. Memoirs of Ehime University (2B) 4: 85–172.

Price L (2016) An introduction to some cave fauna of Malaysia and Thailand. Acta Carsologica 33: 311–317. https://doi.org/10.3986/ac.v33i1.359

Ran JC, Yang WC (2015) A review of progress in Chinese troglofauna research. Journal of Resources and Ecology 6: 237–246. https://doi.org/10.5814/j.issn.1674-764x.2015.04.007

Rong L, Yang L (2004) Biodiversity of Guizhou Province and its karst environment. Journal of Guizhou Normal University (Natural Sciences) 2004, (04): 1–6 (in Chinese with English abstract). https://doi.org/10.3969/j.issn.1004-5570.2004.04.001

Schawaller W (1995) Review of the pseudoscorpion fauna of China (Arachnida: Pseudoscorpionida). Revue Suisse de Zoologie 102: 1045–1063. https://doi.org/10.5962/bhl.part.80489

Sket B (2008) Can we agree on an ecological classification of subterranean animals? Journal of Natural History 42: 1549–1563. https://doi.org/10.1080/00222930801995762

Song Y, Zhao HF, Luo YF, Li SQ (2017) Three new species of *Pinelema* from caves in Guangxi, China (Araneae, Telemidae). ZooKeys 692: 83–101. https://doi.org/10.3897/zookeys.692.11677

Stone FD, Howarth FG (2007) Hawaiian cave biology: status of conservation and management. Proceedings of the 2005 National Cave and Karst Management Symposium; Albany, New York, October 31 - November 4, 2005. Pp. 21–26.

Taylor SJ, Krejca J, Smith JE, Block VR, Hutto F (2003) Investigation of the potential for red imported fire ant (*Solenopsis invicta*) impacts on rare karst invertebrates at Fort Hood, Texas: A field study. In Illinois Bexar County Karst Invertebrates Draft Recovery Plan Natural History Survey. Center for Biodiversity Technical Report, vol. 28. Pp. 1–153.

Tian MY, Huang SB, Wang DM (2017) Discovery of a most remarkable cave-specialized trechine beetle from southern China (Coleoptera, Carabidae, Trechinae). ZooKeys 725: 37–47. https://doi.org/10.3897/zookeys.725.21040

Tian MY, Huang SB, Wang DM (2018) Occurrence of hypogean trechine beetles in Hanzhong Tiankeng Cluster, southwestern Shaanxi, China (Coleoptera: Carabidae: Trechinae). Annales de la Société entomologique de France (N.S.) 54 (1): 81–87. https://doi.org/10.1080/00379271.2017.1417056

Tian MY, Huang SB, Wang XH, Tang MR (2016) Contributions to the knowledge of subterranean trechine beetles in southern China's karsts: five new genera (Insecta: Coleoptera: Carabidae: Trechini). ZooKeys 564: 121–156. https://doi.org/10.3897/zookeys.564.6819

Tilman D, May RM, Lehman CL, Nowak MA (1994) Habitat destruction and the extinction debt. Nature 371: 65–66. https://doi.org/10.1038/371065a0

Trajano E (2000) Cave faunas in the Atlantic tropical rain forest: Composition, ecology and conservation. Biotropica 32: 882–893. https://doi.org/10.1111/j.1744-7429.2000.tb00626.x

van Beynen P, Townsend K (2005) A disturbance index for karst environments. Environmental Management 36: 101–116. https://doi.org/10.1007/s00267-004-0265-9

Vellend M, Verheyen K, Jacquemyn H, Kolb A, Van Calster H, Peterken G, Hermy M (2006) Extinction debt of forest plants persists for more than a century following habitat fragmentation. Ecology 87: 542–548. https://doi.org/10.1890/05-1182

Voituron Y, de Frapoint M, Issartel J, Guillaume O, Clobert J (2010) Extreme lifespan of the human fish (*Proteus anguinus*): A challenge for ageing mechanisms. Biology Letters 7: 105–107. https://doi.org/10.1098/rsbl.2010.0539

Whitten T (2009) Applying ecology for cave management in China and neighboring countries. Journal of Applied Ecology 46: 520–523. https://doi.org/10.1111/j.1365-2664.2009.01630.x

Wynne JJ, Howarth FG, Sommer S, Dickson BG (2019) Fifty years of cave arthropod sampling: techniques and best practices. International Journal of Speleology 48: 33–48. https://doi.org/10.5038/1827-806X.48.1.2231

Zhou ZF, Zhang SY, Xiong KN, Li B, Tian ZH, Chen Q, Yan L, Xiao SZ (2017) The spatial distribution and factors affecting karst cave development in Guizhou Province. Journal of Geographical Sciences 27 (8): 1011–1024. https://doi.org/10.1007/s11442-017-1418-0